AD-A184 666 AN APPLICATION OF A GRADIENT RELAXATION METHOD TO NOISY INFRARED IMAGES(U) NAVAL POSTGRADUATE SCHOOL MONTEREY CA J C MCDOUGALL JUN 87 1/2

UNCLASSIFIED F/G 17/5 1 NL

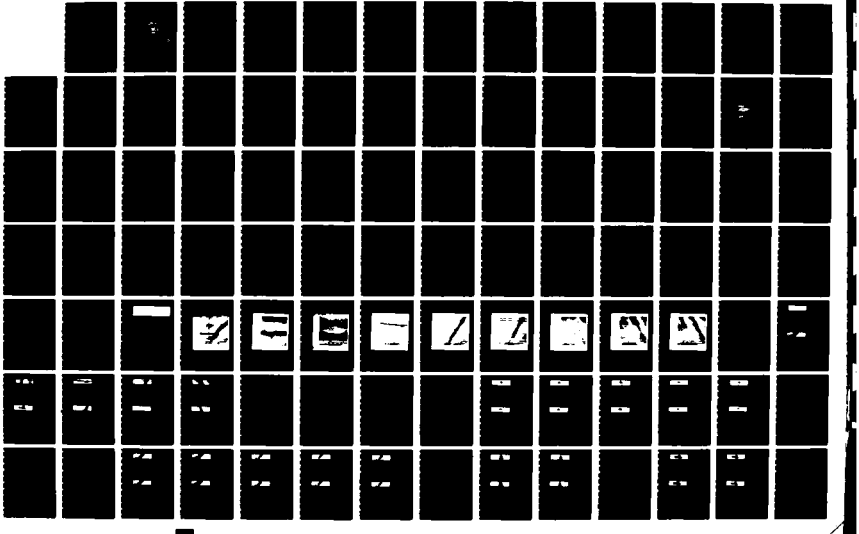

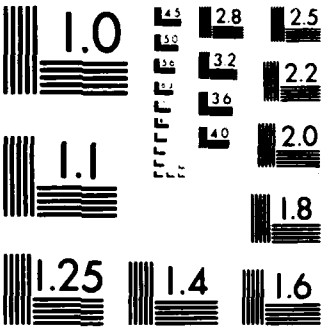

NAVAL POSTGRADUATE SCHOOL
Monterey, California

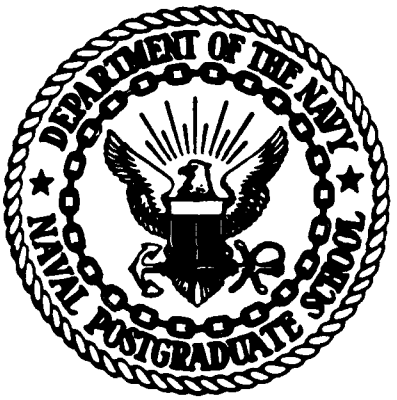

THESIS

AN APPLICATION OF A GRADIENT RELAXATION METHOD TO NOISY INFRARED IMAGES

by

James Chauncy McDougall

June 1987

Thesis Advisor: Chin-Hwa Lee

SECURITY CLASSIFICATION OF THIS PAGE

REPORT DOCUMENTATION PAGE

1a REPORT SECURITY CLASSIFICATION UNCLASSIFIED	1b RESTRICTIVE MARKINGS
2a SECURITY CLASSIFICATION AUTHORITY	3 DISTRIBUTION/AVAILABILITY OF REPORT Approved for public release; distribution is unlimited.
2b DECLASSIFICATION/DOWNGRADING SCHEDULE	
4 PERFORMING ORGANIZATION REPORT NUMBER(S)	5 MONITORING ORGANIZATION REPORT NUMBER(S)
6a NAME OF PERFORMING ORGANIZATION Naval Postgraduate School 6b OFFICE SYMBOL (If applicable) 62	7a NAME OF MONITORING ORGANIZATION Naval Postgraduate School
6c ADDRESS (City, State, and ZIP Code) Monterey, California 93943-5000	7b ADDRESS (City, State, and ZIP Code) Monterey, California 93943-5000
8a NAME OF FUNDING/SPONSORING ORGANIZATION 8b OFFICE SYMBOL (If applicable)	9 PROCUREMENT INSTRUMENT IDENTIFICATION NUMBER
8c ADDRESS (City, State, and ZIP Code)	10 SOURCE OF FUNDING NUMBERS PROGRAM ELEMENT NO / PROJECT NO / TASK NO / WORK UNIT ACCESSION NO

11 TITLE (Include Security Classification)
AN APPLICATION OF A GRADIENT RELAXATION METHOD TO NOISY INFRARED IMAGES

12 PERSONAL AUTHOR(S)
McDougall, James C.

13a TYPE OF REPORT	13b TIME COVERED	14 DATE OF REPORT (Year Month Day)	15 PAGE COUNT
Master's Thesis	FROM _____ TO _____	1987 June	119

16 SUPPLEMENTARY NOTATION

17 COSATI CODES			18 SUBJECT TERMS (Continue on reverse if necessary and identify by block number)
FIELD	GROUP	SUB-GROUP	Digital Image Processing, Pattern Recognition, Segmentation

19 ABSTRACT (Continue on reverse if necessary and identify by block number)

Image segmentation is an essential preliminary step in automatic pictorial pattern recognition and scene analysis problems. The objective of segmentation techniques is to partition an image into regions or components. The purpose of this thesis is to analyze a segmentation technique called gradient relaxation. The gradient relaxation method is a viable method in segmenting objects within an image. The gradient relaxation technique is applicable to images having unimodal distributions. This method is applied to noisy infrared images in an attempt to detect and classify the target. The method allows for an easy selection of a threshold value which may be required for other types of

20 DISTRIBUTION/AVAILABILITY OF ABSTRACT ☒ UNCLASSIFIED/UNLIMITED ☐ SAME AS RPT ☐ DTIC USERS	21 ABSTRACT SECURITY CLASSIFICATION UNCLASSIFIED
22a NAME OF RESPONSIBLE INDIVIDUAL Chin-Hwa Lee	22b TELEPHONE (Include Area Code) (408) 646-2082 22c OFFICE SYMBOL 62LE

DD FORM 1473, 84 MAR 83 APR edition may be used until exhausted
All other editions are obsolete

SECURITY CLASSIFICATION OF THIS PAGE

19. ABSTRACT (continued)

image processing on the image. The main issue is to examine the effectiveness of this technique applied to noisy infrared images from uncooled focal plane array sensor having unimodal distributions. The technique was able to extract the target in the image, producing a homogeneous and uniform region for most of the cases studied. A target which was fragmented into several parts because of the noise is not detectable. The technique could be implemented in hardware and applied to the inputs of a classification system for detectable objects in noisy infrared images.

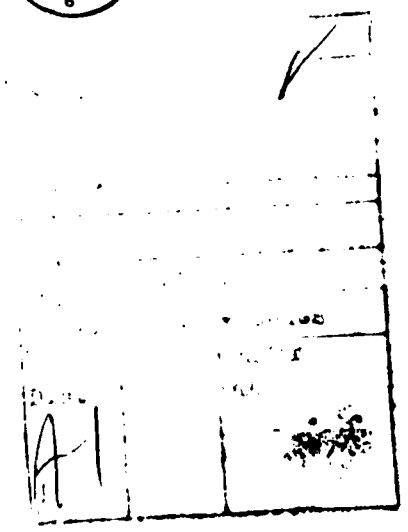

Approved for public release; distribution is unlimited.

An Application of a Gradient Relaxation Method To Noisy Infrared Images

by

James Chauncy McDougall
Captain, United States Army
B.S.E.E., University of Texas at El Paso, 1980

Submitted in partial fulfillment of the requirements for the degree of

MASTER OF SCIENCE IN ELECTRICAL ENGINEERING

from the

NAVAL POSTGRADUATE SCHOOL
June 1987

Author: James C McDougall
James Chauncy McDougall

Approved by: Chin-Hwa Lee
Chin-Hwa Lee, Thesis Advisor

Charles W. Therrien
Charles W. Therrien, Second Reader

John P. Powers, Chairman,
Department of Electrical and Computer Engineering

Gordon E. Schacher
Dean of Science and Engineering

ABSTRACT

Image segmentation is an essential preliminary step in automatic pictorial pattern recognition and scene analysis problems. The objective of segmentation techniques is to partition an image into regions or components. The purpose of this thesis is to analyze a segmentation technique called gradient relaxation. The gradient relaxation method is a viable method in segmenting objects within an image. The gradient relaxation technique is applicable to images having unimodal distributions. This method is applied to noisy infrared images in an attempt to detect and classify the target. The method allows for an easy selection of a threshold value which may be required for other types of image processing on the image. The main issue is to examine the effectiveness of this technique applied to noisy infrared images from uncooled focal plane array sensor having unimodal distributions. The technique was able to extract the target in the image, producing a homogeneous and uniform region for most of the cases studied. A target which was fragmented into several parts because of the noise is not detectable. The technique could be implemented in hardware and applied to the inputs of a classification system for detectable objects in noisy infrared images.

TABLE OF CONTENTS

LIST OF TABLES

LIST OF FIGURES

ACKNOWLEDGEMENT

I wish to express my gratitude to my thesis advisor, Dr. Chin-Hwa Lee, in his advice and assistance in the completion of this thesis. I would also like to thank Dr. Charles W. Therrien and others that directly or indirectly contributed in the accomplishment of this thesis. I would also like to acknowledge the Defense Mapping Agency (DMA) for providing the equipment used in the support of this study.

I. INTRODUCTION

A. IMAGE PROCESSING

Image processing is concerned with the extraction of information from natural images which are acquired from image sensors. Information extraction involves the detection and recognition of patterns within the image.

The human eye has an extraordinary pattern recognition capability, being able to discern approximately one hundred shades of gray. However, the eye is not always able to extract all the information from an image due to radiometric degradation, geometric distortion, and noise introduced during recording, transmission, and display of the images. These factors can severely limit recognition of patterns or objects. One purpose of image processing is to aid the human eye in extracting the desired image by removing these distortions.

Three methods are available in performing image processing operations: digital, optical, and photographic. Black and white film can retain a limited range of gray level intensities (50 or less), whereas digital computers can represent several hundreds or thousands of gray levels. [Ref. 1] Optical methods are faster, but do not offer the flexibility of digital methods. Flexibility is limited by

such factors as the compromise between computation time and the accuracy of the results. [Ref. 2] Computers can be used to apply various linear and nonlinear transformations to images which cannot be performed optically. Digital information extraction techniques can fully exploit the statistical nature of digital imagery. These techniques can also be used for analysis based on correlation of image data with nonimaging data. This includes correlation of remotely sensed imagery with nonimaging georeferenced cartographical data bases.

The digital computer, used in numerically oriented analysis because of its quantitative character and great speed, has become a key tool. Numerically oriented remote sensing takes advantage of the computer to emphasize the inherently quantitative aspects of the image data, dealing with the data rather abstractly as a collection of measurements rather than as an image. Tremendous quantities of data are of real value only when the data can be acquired and analyzed both rapidly and cost effectively. The growth of digital computer technology has enabled the development of digital image processing techniques. Because of faster and cheaper computational components, large-capacity high-density digital data storage devices, and improved display technology, the processing, manipulation, and display of

large volumes of digital imagery has become possible. [Ref. 3]

A digital image processing system contains three main elements as shown in Figure 1.1 and are defined as follows:

Figure 1.1: Image Processing System

(1) Image Acquisition. This involves the conversion of a scene into a digital representation. This element can be performed by a sensor system which is designed to view a scene and provide a digital representation of it. The acquisition involves the conversion of an image from a television signal or film into a digital representation. [Ref. 3] An image sensor can be characterized by a number of features, including:

- signal-to-noise ratio - a measure of the useful information extracted from the sensor's signal;

- dynamic range - variation in the range of the response to light energy;
- resolution - measure of the smallest detail in the image which can be retained by the sensor;
- transfer function - relationship between incoming light spatial frequency and output spatial frequency;
- integration time - the time in which the sensor accumulates charges generated by the incoming light;
- reading speed - the scanning time for a given total spatial resolution and picture size;
- spectral sensitivity - the portion of the electromagnetic spectrum to be used by the sensor. [Ref. 4]

The sophistication of the acquisition system based on the above features and capabilities will greatly affect the cost, performance, and reliability of the acquisition system. However, no matter how sophisticated the system is, certain degradations will be introduced into the image. These degradations fall into two categories: radiometric and geometric distortions. Radiometric degradations occur from blurring affects of the imaging system, nonlinear amplitude responses, shading, transmission noise, atmospheric interference (scattering, attenuation, haze), variable surface illumination (differences in terrain slope and orientation), and change of terrain radiance with viewing angle. Geometric distortions can be categorized into three

categories: sensor-related such as aberrations in the optical system, or nonlinearities and noise in the scan-deflection system; sensor-platform related caused by attitude and altitude of the sensor; and object-related distortions caused by Earth rotation and curvature, and terrain relief. [Ref. 1]

(2) Image Processing. This element provides the digital processing of the image or images to produce a desired result (Figure 1.2). This processing can range from simple enhancement of an image for better display of scene detail to more complex processing involving several component images. [Ref. 3] Digital image processing techniques can be divided into two different groups. The first group includes quantitative restoration of images to correct for degradation and noise, registration for overlaying and mosaicing, and subjective enhancement of image features for interpretation. The second group is concerned with the extraction of information from the images. This area of analysis includes object detection, segmentation of images into characteristically different regions, and determination of structural relationships among the regions. [Ref. 1] Within these two groups fall two categories: subjective and quantitative processing.

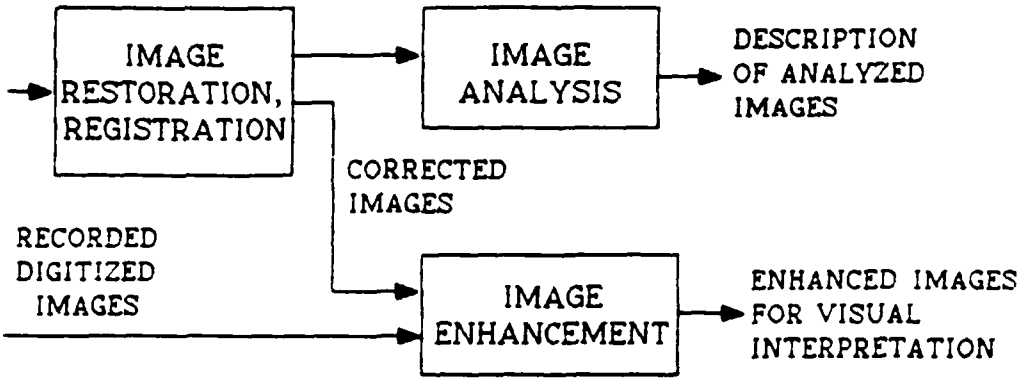

Figure 1.2: Image Processing Steps. [Ref. 1]

Subjective processing is usually performed in an adaptive, interactive, and iterative manner. It is a trial and error process, and success is based on the ability of the observer to detect information of interest in the final or enhanced image. The changes achieved in the 'before' and 'after' versions of the images processed subjectively are often quite dramatic, despite the relative computational simplicity of many of the subjective techniques. A basic tool which is used in performing subjective enhancement and image analysis is the histogram. The histogram reveals the distribution of the intensities within the image; it is represented graphically as a plot of the number of picture elements (pixels) at a given intensity, versus the gray level intensity. Quantitative techniques are generally performed on an

image in a nonadaptive, noninteractive manner. The processing method is based on a predefined mathematical algorithm, and success in processing is based on the correctness of the model. Examples of qualitative processing is the removal of radiometric and geometric distortions. [Ref. 3]

This element can reduce some of the requirements of the image acquisition system, such as signal to noise ratio, dynamic range, transfer function, integration time, and reading speed. By reducing some of the requirements, the cost of the acquisition system can be reduced, and the money saved can be used to improve the processing capabilities of the complete imaging system.

(3) Image Display. The final element provides for generation of an output product that can be seen by a human observer. This element provides the required conversion of digital data into an analog form. Processed images can be viewed on a volatile display monitor that presents the digitized data in an analog form (video signal). The imagery data can be recorded on film or other hard copy format. [Ref. 3]

B. OVERVIEW

This thesis is concerned with the image processing step and specifically with image analysis using segmentation

techniques. The segmentation technique used here is called the gradient relaxation method. This method utilized an iterative probability adjustment process to segment pixels into two regions, 'light' and 'dark'. This method is highly dependent on the selection of weighting factors. They determine the speed at which the segmentation process coverages and to regions pixels will be assigned. Analysis is done on noisy infrared images of ships to determine if targets can be detected, and/or classified. Detection is the ability of the observer to sense that an object of interest is in the field of view. Classification is defined (in the military sense) as the ability of the observer to identify the detected object as to its type. For Army operations, classification could be a tank, truck, or helicopter. For Naval operations, a large ship, small ship, combatant, or merchant vessel would be typical types. At different steps of engagement, the need to detect or to classify the object will depend upon the situation.

Chapter II is a survey of contemporary image segmentation techniques. These techniques are classified into three categories: characteristic feature thresholding, edge detection, and region extraction. The specific algorithm which is investigated in this thesis is a combination of feature thresholding and region extraction, using a relaxation or iterative process for the segmentation

of the image. Chapter III is a discussion on the gradient relaxation algorithm, the particular method used in this investigation. This chapter introduces the relaxation process and develops the gradient relaxation algorithm. This algorithm is applied to several noisy infrared images of ships in Chapter IV. An analysis is done on how effective the algorithm is in reducing or eliminating noise, the ability to detect and classify an object in the field of view. The final chapter summarized the results, discusses possible applications, implementation of the algorithm, and possible future work.

II. TECHNIQUES USED IN SEGMENTATION

A. SEGMENTATION BASICS

A major branch of image processing deals with image analysis or scene analysis, where the input is pictorial, but the output is a description of the given picture or scene. The following are examples of image analysis problems:

(1) The input is text and it is desired to read the text; here the description of the input consists of a sequence characters.

(2) The input is a nuclear bubble chamber picture, and it is desired to detect and locate certain events (e.g., particle collisions); the description consists of a set of coordinates and names of event types.

(3) The input is a picture of a miotic cell and the output is a 'map' showing the arrangement of the chromosomes in a standard order. This output requires knowledge of the location and identification of the chromosomes.

(4) The input is an aerial photograph of terrain with the desired output being a map showing specific types of terrain feature (vegetation, buildings, ships, roads, etc.). The construction of this output also requires

the location and identification of the desired terrain features. [Ref. 5]

In all of these examples, the description refers to specific parts or objects in the picture in terms of their properties and the relationships between the objects. Image analysis consists of four steps:

Step 1: Segmentation - This is the partitioning of an image into different regions, each having different properties.

Step 2: Regional descriptions - This procedure is used to characterize the segmented regions by a set of descriptors which are not sensitive to such variations as changes in size, rotation, or translation. These descriptors will bring out features which will aid in differentiating regions with different attributes.

Step 3: Relational descriptions - This procedure deals with the organization of these regions into a meaningful structure.

Step 4: Descriptions of similarity - The final step deals with the problem of establishing measures of similarity between regions in an image. [Ref. 6]

Image segmentation is a critical step in the image analysis process because errors in segmentation might propagate through the other processes producing an incorrect

description of the scene. The question can then be asked, what should a good image segmentation be? Regions of an image segmentation should be uniform and homogeneous with respect to some characteristic such as gray level or texture. Region interiors should be simple and contain few gaps or holes. Adjacent regions of a segmented image should be significantly different in value with respect to the characteristic on which the regions are homogeneous. Boundaries of each region should be smooth and spatially accurate. Achieving these desired properties is difficult because precisely uniform and homogeneous regions are typically full of small holes and have jagged boundaries. Requiring that adjacent regions have a large difference in value can cause regions to merge and/or boundaries to be lost. All of these effects introduce errors which are undesirable. [Ref. 7]

There is neither a standard approach to nor theory for of image segmentation. Segmentation techniques are basically ad-hoc and differ in the way each emphasizes one or more of the properties discussed previously. In the way each strikes a balance between one desired property and another property. T. Pavlidis has commented that an image segmentation problem is basically one of psychophysical perception and therefore not susceptible to a purely analytical solution. Any mathematical algorithm must be

supplemented with heuristics, involving semantics about the class of images under consideration. Quite often, simple heuristics are not enough, and it is essential to introduce a priori knowledge about the image. An example of this is the dalmatian dog picture (Figure 2.1). Without the priori knowledge that a picture consists of a dalmatian dog, most human observers would perceive the picture as pure noise. However, if the observers are told that the image consists of a dalmatian dog, most will identify the dog in the picture. [Ref. 8]

Figure 2.1: This picture is perceived to be random noise. Mention 'dalmatian dog' and that image will be seen. [Ref. 8]

Almost all segmentation techniques are based on either the concept of similarity (e.g., characteristic feature

clustering) or discontinuity (e.g., edge detection). These techniques can be categorized into three areas: (1) characteristic feature thresholding or clustering, (2) edge detection, and (3) region extraction. [Ref. 9] These techniques are discussed in the following sections.

B. CHARACTERISTIC FEATURE THRESHOLDING

Characteristic feature or gray-level thresholding is a widely used segmentation technique. The general idea is to divide the gray scale of a histogram into bands of a similar characteristic, e.g., gray level. In general, thresholding can be described mathematically as

$$S(x,y)=k \text{ if } T_{k-1} < f(x,y) < T_k,\ k=1,2,\ldots,m$$

where (x,y) are the x- and y-coordinate of a pixel; S(x,y) is the segmented function of (x,y); $T_1,\ldots,T_m$ are the threshold values with T_1 being the minimum and T_m being the maximum; m is the total number of distinct bands (or labels) assigned to the segmented image. The selection of the threshold value(s) is not a simple task and can be dependent on several factors. If the threshold depends only on f(x,y), the gray level, it is called a 'global threshold'. If the value is dependent on f(x,y) and the average gray level of the neighborhood around that pixel, it is called a 'local threshold'. If the threshold is based on the gray level f(x,y), the neighborhood gray level, and the coordinates x and y of the pixel, it is called a 'dynamic

threshold'. [Ref. 9] As can be seen, the selection of a threshold value is not an easy task, but the selection of the threshold is very important.

There are several methods to select a global threshold. Some are based on the gray level histogram, others on local properties such as the gradient, or Laplacian of an image, and others for an image consisting of an object and background where the percent of the object area in the image is known. The 'mode method' is a technique based on the gray level histogram where the threshold is selected in the valley between the peaks (or modes) of the histogram. This approach has the advantage that it reduces the probability of misclassifying an object point as a background point and vice versa.

However, there are some disadvantages to this technique. Spatial information is not used to arrive at the thresholds which means there is no assurance that the segmented regions are contiguous. The minimum location of the valley may be difficult to locate since the valley may be broad and flat. Methods have been proposed to sharpen the peaks to more clearly define a valley bottom. A. Rosenfeld [Ref. 10] proposed an iterative method, called relaxation, to sharpen the peaks in enhancing images and their histograms. [Ref. 9]

A simple example of a bimodal (two peaks) histogram is shown in Figure 2.2. The objective is to select T such that

band B_1 contains, as closely as possible, levels associated with the background, while B_2 contains levels associated with the object(s). Each band is assigned a single gray level within that band which will best discriminate the object from the background. This figure also demonstrates the case of a broad and flat valley, where many of the pixels in band B_2 are not part the object but may be noise, therefore part of the background. The iterative method mentioned above is a possible solution to enhancing the peak at the right creating a truer representation of the object. Using the original threshold value, errors will be introduced into the scene analysis process, which is unacceptable as was stated earlier. This thesis looks at the use of the iterative method in selecting a threshold and creating a segmented image.

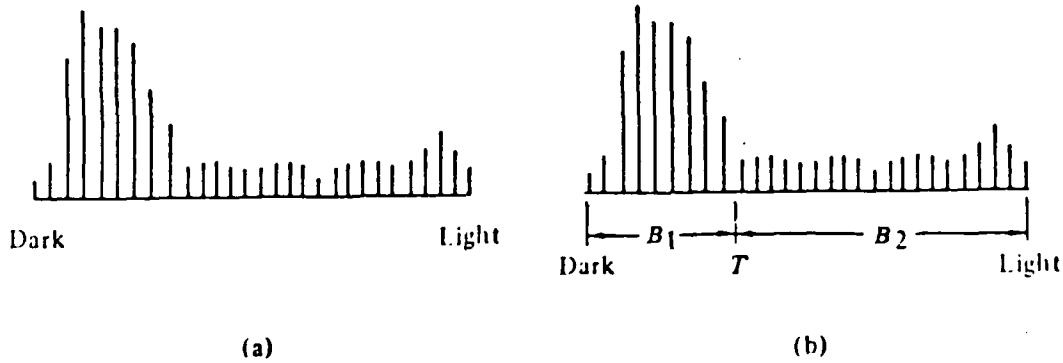

Figure 2.2: Histogram thresholding [Ref. 6]

C. EDGE DETECTION

Edge detection is an image segmentation technique based on the discontinuity of gray levels at the boundary between different objects. This discontinuity can be any one of several geometrical forms:

(1) An edge - The gray level is uniformly consistent in each of two adjacent regions, and changes abruptly at the border between the regions.

(2) A line or curve - The gray level of a thin strip in the image differs from the two regions on either side of the strip.

(3) A spot - The gray level is relatively constant except at one location in the image. This looks like a spike in a cross-sectional view (Figure 2.3), but appears as a spike from all directions. [Ref. 5]

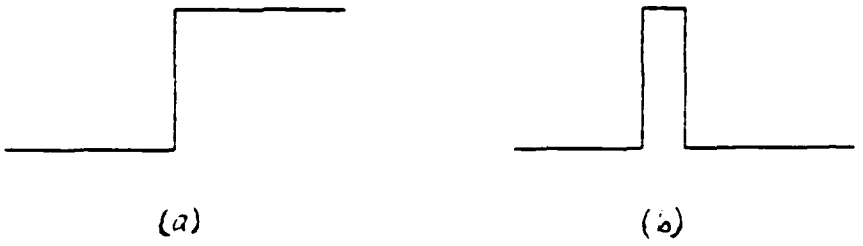

Figure 2.3: a) Idealized edge cross section.
b) Perfect 'spike' line.

Edge detection schemes consist of three steps:

(1) The use of a gradient or derivative operator to detect locations where the gray level is changing rapidly. In the case of digital images, difference operators are used instead of derivatives.

(2) A threshold operation is performed on the gradient in order to decide if an edge has been found. The edge points are assigned a value greater than the background if the gradient is larger than a certain threshold. This threshold selection is a key problem in noisy images. Too high a threshold does not permit the detection of subtle, low-intensity edges. A value too low causes noise to be detected as edges.

(3) Pixels which have been determined to be edges must then be linked to form closed curves surrounding the regions. [Ref. 11]

Edge detection is of limited value as an approach to segmentation of noisy remotely sensed images. Often the edges have gaps at places where the transition between regions are not sufficiently abrupt. Additional edges may be detected at points that are not part of region boundaries, and the detected edges will not form a set of closed, connected object boundaries. [Ref. 1]

D. REGION EXTRACTION

Another way of doing segmentation is to divide the image into regions. Region extraction techniques can be divided into three categories: (1) region merging, (2) region splitting, and (3) combination of region merging and splitting.

Since the goal of segmentation is to partition an image into regions, a direct approach is to attempt a partitioning of the image into regions which satisfy a similarity criterion, i.e., group points into regions. The criteria which can be used in extracting objects include region homogeneity (in gray level, texture, etc.) and contrast with the background, strength of the region's edges, size, shape simplicity, and conformity to a desired texture or shape. The advantage of this approach is that it results not only in boundary point of regions but also in satisfying a similarity criterion for all points within the regions. In order to group points, three fundamental issues must be resolved. The first is to determine the number of regions. The second is to determine some properties or features which distinguish one region from the other regions. The third is to specify a suitable similarity criterion which will produce a 'meaningful' segmentation. A 'meaningful' segmentation is a subjective term and is based on subjective methods. [Ref. 6]

One method is called region growing. This approach starts with very small regions with uniform pixel properties. Growth begins by starting with one of these regions and merging neighboring regions with it, one at a time. The choice of which neighbor to merge will depend on both the similarity of the regions (based on gray level, texture, etc.) and on the size and shape of the resultant merged region. Because of the sequential operations involved, the process is slow.

Another approach is region splitting. This approach considers the whole image as a single region, and partitions it by repeated splitting. Two simple approaches of subdividing an image are bisection and triangulation. In bisection, if the complete image is not homogeneous, it is divided into quadrants; if a quadrant is not homogeneous, it is divided again into quadrants; this process continues until all of the quadrants are homogeneous. In triangulation, the image is divided into four triangular sectors which meet at a point having a gray level farthest from the mean; if a triangle is not homogeneous, it is divided into four triangles; this continues in a similar manner as in the bisection method. There are two serious problems with this technique. The image could be subdivided down to the single pixel level, which is probably

unacceptable, or the final partition may contain adjacent regions with identical characteristics.

A method which is preferable to either merging or splitting is the combination of the two, or the merge-and-split method. The general idea is to start with a given initial partition; the entire image is a region, each pixel or a small block of pixels is a region. Adjacent regions are merged if the new region is sufficiently homogeneous, and a region will be split if it is not considered to meet a homogeneous criteria. [Ref. 5]

One of the disadvantages of region merging processes is their inherently sequential nature. The regions produced depend greatly on the order in which regions are merged together. Most, if not all region extraction methods rely heavily on local information. It is difficult to incorporate global information into an algorithm unless the category of pictures to be processed is severely limited. All region extraction techniques process pictures in an iterative manner which usually involves a large expenditure of computational time and memory.

A method which takes advantage of both parallel and sequential methods is called relaxation. 'Parallel' methods have the classification decision done at each point independently of the decisions at other points. 'Sequential' methods are those which base their decision on

previous decisions. 'Sequential' methods are more powerful than 'parallel' methods because they learn to better define the region classification as they proceed. However, 'sequential' methods are slower and their results are still dependent on the order in which the points are processed. [Ref. 9]

Relaxation is an iterative approach which makes probabilistic classification decisions at every pixel in parallel at each iteration. It then adjusts these decisions at successive iterations based on the decisions made at the preceding iteration at the neighboring points. The relaxation method is conducive to the segmentation problem in noisy infrared images. Noise within or near the target will be filtered out due to the sequential process involved when the probability classification of the noise pixel is adjusted based on its neighbors. The adjustment of the pixels to a high probability ('light') or a low probability ('dark') will enhance the peaks in the histogram, allowing for an easy selection of a threshold. The theory for this method will be discussed more fully in the next chapter. [Ref. 5] In order to evaluate the usefulness of this method, experiments are conducted and the results presented in Chapter IV.

III. SEGMENTATION BY THE GRADIENT RELAXATION METHOD

Segmentation of an image into regions can be done by various methods described in the previous chapter. These techniques fall into several categories: region merging, region splitting, and a combination of merging and splitting as mentioned before. A method which provides for an easy selection of a threshold value and combines the advantages of sequential and parallel processing techniques is the relaxation technique. This chapter will discuss the theory behind the relaxation technique and develop the mathematical relationships used in the gradient relaxation method, the segmentation technique used in this work.

A. INTRODUCTION TO RELAXATION PROCESSES

Relaxation, or iterative methods, were originally developed as a numerical analysis tool to solve a set of simultaneous equations. In recent years, relaxation methods have been applied to image analysis. The classification of parts in an image using relaxation techniques was first introduced by A. Rosenfeld [Ref. 12] and S. Zucker [Ref. 13]. These methods have been applied to histogram modification (a peak enhancement scheme), noise cleaning, edge and curve detection, curve thinning, angle detection, template matching, and region labeling.

Image analysis usually involves the discrimination or classification of parts within an image. Classification can be based on gray level intensity by categorizing points as 'light' (object) or 'dark' (background), or vice versa, in the segmented infrared images. For edge or non-edge point classification, it is based on some local property (e.g., the magnitude of the gradient) evaluated at that point. Angles on a curve are classified based on the magnitude of the curvature of the curve at that point. Classification of image points based on these properties is error-prone, because noise in the image may cause the local property to be misleading. This misclassification can be compounded if the classification is done in a 'parallel' fashion, i.e., each point is classified without reference to any classification decisions of is neighboring points. However, if the classification procedure has sequential operations, the process takes advantage of previous classification of the neighbor points. This is the basis of the classification of objects using relaxation methods. The iterative approach has two advantages: (1) classification decisions become better informed as the analysis proceeds and (2) the method can use fuzzy or probabilistic classifications rather than making firm decisions immediately as would be the case in a parallel process. [Ref. 10]

The iterative probabilistic classification method can be described in the following manner. A set of objects (points, lines, regions, etc.) $A_1, A_2, \ldots, A_N$ are classified into a set of classes $\lambda_1, \lambda_2, \ldots, \lambda_m$. Each object has a neighbor relation, i.e., each A_i has a specified set of A_j's as neighbors. Each object A_i is associated with a probability vector $(P_{i1}, P_{i2}, \ldots, P_{im})$ where P_{ik} is an estimate of the probability that A_i belongs to a certain class λ_k. The initial probability is based on a conventional type of analysis. For example, a point's probability is based on its gray level, i.e., proportional to the distances of that gray level to the maximum values of the gray level range. The next step is to define a measure of compatibility between an object A_i belonging to λ_h, and another object A_j belonging to λ_k. If there is a high compatibility (or similarity) between object A_i and object A_j, i.e. $(A_i, A_j \varepsilon \lambda_k)$, object A_i is reinforced by its neighbors. Thus its probability is increased. However, if the objects are incompatible, the probability remains the same or decreases. [Ref. 10] This can be expressed mathematically as

$$P_{ih} = \frac{(P_{ih})(1 + Q_{ih})}{(\sum_{h}(P_{ih})(1 + Q_{ih}))}$$

where q_{ih}, a compatibility vector, is defined as

$$Q_{ih} = \sum_{jk}^{Nm} \Sigma c(i,h,j,k) P_{jk}$$

where c(i,h,j,k) is the compatibility coefficient between object A_i and A_j, with values between [-1,1] (low compatibility, high compatibility). [Ref. 14]

The application of relaxation techniques to segmentation involves the classification of pixels into 'light' and 'dark' classes. The initial probabilities of each pixel in a certain class is based on its gray level, i.e., proportional to the distances of the gray level to the maximum value of the gray level range. These probabilities are iteratively adjusted based on the neighborhood probabilities, with 'light' reinforcing 'light' and 'dark' reinforcing 'dark'. This is the basic technique used in the algorithm which will be discussed in the following section.

B. GRADIENT RELAXATION ALGORITHM

1. Gradient Relaxation Basics

The segmentation technique which is to be analyzed is a region splitting method using a recursive procedure of the two-class relaxation technique. The two-class technique controls the segmentation process and provides for an automatic selection of a threshold. Normally, in the application of various segmentation techniques based on thresholding, the histogram shows two or more peaks in at least one of the spectral features corresponding to various homogeneous regions of an image. Very often preprocessing is done to alter the histograms and local properties are

used to compute the local, global, or dynamic threshold. However, if the intensity histogram of the image is unimodal, then the application of thresholding techniques produces a poor segmentation and does not establish a criteria for automatic threshold selection. A unimodal distribution is typically obtained when the image consists mostly of a large background area with other small but significant objects (or regions) in the image. For example, in the case of a complex aerial photographs which may have many objects within the scene, the histogram may have only one broad peak because the restricted range of intensities for the objects is probably covered by the background.

2. Development of the Gradient Relaxation Algorithm

In a paper by B. Bhanu and O. Faugeras [Ref. 15], they proposed a gradient relaxation algorithm for the segmentation of images having an unimodal distribution. This algorithm is based on the use of inconsistency and uncertainty to define a global criterion upon the set of pixels. Let λ_1 and λ_2 correspond to two classes, white (gray level = 255) and black (gray level = 0), respectively. 'Inconsistency' is defined as the difference between the probability vector $\mathbf{P}_i = [P_i(\lambda_1), P_i(\lambda_2)]$, and the compatibility vector $\mathbf{Q}_i = [Q_i(\lambda_1), Q_i(\lambda_2)]$, of the ith pixel. In other words, what is the discrepancy between what every pixel 'thinks' about its own labeling and what its

neighbors 'think' about that labeling (Q_i). 'Uncertainty', is measured by the entropy function and is defined to be

$$H_i(P_i(\lambda_1)) = \frac{1}{\ln 2}\left[P_i(\lambda_1)\ln\frac{1}{P_i(\lambda 1)} + P_i(\lambda_2)\ln\frac{1}{P_i(\lambda_2)}\right] \qquad (3.1)$$

A criterion is defined as

$$C(P_1,P_2,\ldots,P_N) = \sum_{i=1}^{N} P_i \cdot Q_i \qquad (3.2)$$

where N is the total number of pixels in the image. The goal is to maximize this criterion. The relaxation process is specified by choosing a model of interaction between pixels and attach to each pixel i the set V_i of its eight nearest neighbors. The idea is to make like pixels reinforce like pixels by defining a compatibility function c,

$$c(i,\lambda_m,j,\lambda_n)=0 \quad m\neq n, \text{ for pixel } j \text{ in } V_i \text{ for all } i$$
$$c(i,\lambda_m,j,\lambda_m)=1 \quad m=1,2 \text{ for pixel } j \text{ in } V_i \text{ for all } i \qquad (3.3)$$

where i ranges from 1 to N pixels.

The compatibility vector, Q_i, for the two class case is then

$$Q_i(\lambda_m)=1/8 \sum_{j\varepsilon V_i} \sum_{m=1}^{2} c(i,\lambda_m,j,\lambda_n)P_j(\lambda_n) \quad m=1,2 \ , \ i=1,\ldots,n \qquad (3.4)$$

Substituting for c, this becomes the mean neighborhood probability of the ith pixel for the case being considered,

$$Q_i(\lambda_m)=1/8 \sum_{j\epsilon V_i} P_j(\lambda_m) \qquad (3.5)$$

The choice of compatibility function in (3.3) will provide the desired result in the interior of the region, but along the edges of a region the pixel label may be uncertain because of two different classes of neighbors. This may cause distortion at the boundary.

The maximization of the criterion (3.2) means that a local maximum has been sought that is close to the initial labeling $P_i^{(o)}$. The maximum criterion is achieved by aligning the vectors $\mathbf{P}_i$ and $\mathbf{Q}_i$ while turning them into unit vectors. This results in increasing the consistency (reducing the difference) and the certainty between the vectors $\mathbf{P}_i$ and $\mathbf{Q}_i$ while turning them into unit vectors. This results in increasing the consistency (reducing the difference) and the certainty between the vectors $\mathbf{P}_i$ and $\mathbf{Q}_i$. It is easily seen from the definition of inconsistency that the minimum occurs when $\mathbf{P}_i = \mathbf{Q}_i$. From Figure 3.1, the maximum entropy, or high uncertainty, occurs when $P_i(\lambda_m) = 0.5$. The maximum certainty occurs when $P_i(\lambda_m) = 0.0$ or 1.0, i.e., $\mathbf{P}_i = [0,1]$ or $[1,0]$, a unit vector.

The uncertainty definition clearly shows that the initial assignment of probabilities is important because it affects the rate of convergence and the final results of the relaxation process. The initial probabilities of each pixel is defined as

$$P_i(\lambda_m) = I(i)/G \qquad (3.6)$$

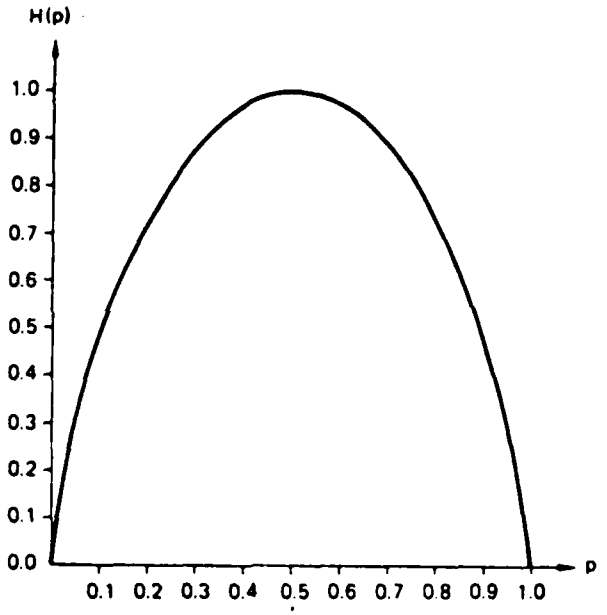

Figure 3.1: Entropy Function [Ref. 16]

where I(i) is the intensity of pixel i in the range $0 < I(i) < G$, and G is the maximum value of the gray levels. This definition disregards any a priori knowledge that may be

known about an image. However, a priori knowledge can be included in the initial probabilities by estimating the ratio of white pixels, N_w, and the number of black pixels, N_b. This ratio is

$$\begin{aligned} r &= N_w/N_b \\ &= \frac{\frac{1}{N}\sum_i P_i(\lambda_1)}{\frac{1}{N}\sum_i P_i(\lambda_2)} \\ &= I/(G - I) \end{aligned} \tag{3.7}$$

where I is the mean intensity level of the image. By knowing this, the distribution of gray levels can be modified so as to make the ratio r closer to the true ratio, r_o. A simple way to do this is to define

$$I'(i) = (FACT)\ (I(i) - I) + I_o \tag{3.8}$$

where I_o is a desired mean and FACT is a parameter which can be chosen to be

$$FACT = 1 \quad \text{for } I(i) > I$$

$$0.7 < FACT < 1.0 \text{ for } I(i) < I$$

Substituting I'(i) in (3.8) into I(i) in (3.6),

$$P_i(\lambda_1) = (FACT)(I(i) - I)/G + I_o/G \tag{3.9}$$

For the analysis performed in this thesis, the following values were used,

$$FACT = 1.0$$

$$G = 255$$

$$I_o/G = 0.5$$

$$P_i(\lambda_1) = (I(i) - I)/255 + 0.5 \qquad (3.10)$$

When the first term of (3.10) is greater than 0.5 or less than -0.5, then a value of 1.0 or 0.0 will be assigned to the probability, respectively. [Ref. 17]

The gradient of the criterion is obtained from (3.2)

$$C = \sum_{i=1}^{N} \mathbf{P}_i \cdot \mathbf{Q}_i$$

$$= P_i(\lambda_1)Q_i(\lambda_1) + P_i(\lambda_2)Q_i(\lambda_2) + \sum_{j \in V_i} \mathbf{P}_j \cdot \mathbf{Q}_j + \sum_{k \notin V_i} \mathbf{P}_k \cdot \mathbf{Q}_k$$

$$\nabla C = \frac{\partial C}{\partial P_i(\lambda_1)}, \frac{\partial C}{\partial P_i(\lambda_2)} \qquad (3.11)$$

Solving for each component of the gradient, we have

$$\frac{\partial C}{\partial P_i(\lambda_1)} = Q_i(\lambda_1) + \frac{\partial}{\partial P_i(\lambda_1)} \sum_{j \in V_i} \mathbf{P}_j \cdot \mathbf{Q}_j \qquad (3.12a)$$

$$\frac{\partial C}{\partial P_i(\lambda_2)} = Q_i(\lambda_2) + \frac{\partial}{\partial P_i(\lambda_2)} \sum_{j \in V_i} \mathbf{P}_j \cdot \mathbf{Q}_j \qquad (3.12b)$$

Looking only at (3.12a) and taking the second term only, we obtain

$$\frac{\partial}{\partial P_i(\lambda_1)} \sum_{j\epsilon V_i} P_j \cdot Q_j = \sum_{j\epsilon V_i} \left(\frac{\partial}{\partial P_i(\lambda_1)} P_j \right) \cdot Q_j + \sum_{j\epsilon V_i} P_j \cdot \left(\frac{\partial}{\partial P_i(\lambda_1)} Q_j \right)$$

The first term is zero because the probabilities of the neighbor pixels, P_j's, are independent of the probability of pixel i, P_i; therefore

$$\frac{\partial}{\partial P_i(\lambda_1)} \sum_{j\epsilon V_i} P_j \cdot Q_j = \sum_{j\epsilon V_i} P_j \cdot \left(\frac{\partial}{\partial P_i(\lambda_1)} Q_j \right)$$

$$= \sum_{j\epsilon V_i} \left[P_j(\lambda_1) \frac{\partial}{\partial P_i(\lambda_1)} Q_j(\lambda_1) + P_j(\lambda_2) \frac{\partial}{\partial P_i(\lambda_1)} Q_j(\lambda_2) \right] \tag{3.13}$$

Recall that the compatibility function (3.5) is

$$Q_j(\lambda_k) = 1/8 \sum_{m\epsilon V_i} P_m(\lambda_k)$$

where V_j is the set of neighbor points of point j, of which point i is a member as shown in Figure 3.2. Taking the partial derivative, we find

$$\frac{\partial}{\partial P_i(\lambda_1)} Q_j(\lambda_1) = 1/8 \frac{\partial}{\partial P_i(\lambda_1)} P_i(\lambda_1)$$

$$= 1/8 \tag{3.14a}$$

and similarly,

$$\frac{\partial}{\partial P_i(\lambda_1)} Q_j(\lambda_2) = 0 \qquad (3.14b)$$

Substituting (3.14) into (3.13) leads to

$$\frac{\partial}{\partial P_i(\lambda_1)} \sum_{j \epsilon V_i} P_j \cdot Q_j = 1/8 \sum_{j \epsilon V_i} P_j(\lambda_1)$$

$$= Q_i(\lambda_1) \qquad (3.15)$$

Substituting (3.15) into (3.12a), results in

$$\frac{\partial C}{\partial P_i(\lambda_1)} = Q_i(\lambda_1) + Q_i(\lambda_r)$$

$$= 2Q_i(\lambda_1)$$

Similarly, the second component is

$$\frac{\partial C}{\partial P_i(\lambda_2)} = 2Q_i(\lambda_2)$$

In summary, the gradient of the criterion, C, is

$$\nabla C = \left[\frac{\partial C}{\partial P_i(\lambda_1)}, \frac{\partial C}{\partial P_i(\lambda_2)} \right]$$

$$\nabla C = \left[2Q_i(\lambda_1), 2Q_i(\lambda_2) \right] \qquad \text{[Ref. 18]} \quad (3.16)$$

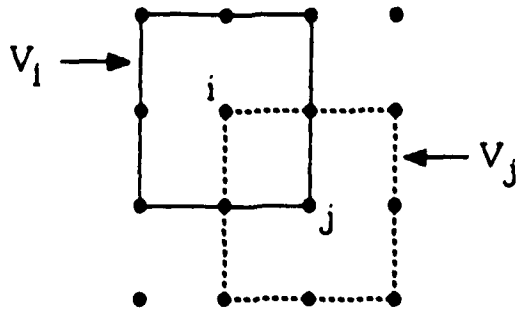

Figure 3.2: Set of pixels V_i and V_j

An efficient method called the steepest ascent technique will be utilized to maximize the criterion. This technique begins with an initial probability, $P_i^{(0)}$, $i = 1,\ldots,N$ for each pixel and iteratively adjusts the probability vector $\mathbf{P}_i$ to converge to a local maximum of criterion (3.2). This is achieved by defining a sequence $\mathbf{P}_i^{(\ell)}$ as:

$$\mathbf{P}_i^{(\ell+1)} = \mathbf{P}_i^{(\ell)} + \rho^{(\ell)} \; \mathrm{PROJ}^{(\ell)} \; \mathbf{G}_I^{(\ell)} \qquad (3.17)$$

where $\rho^{(\ell)}$ is a positive step size, the vector $\mathbf{G}_i^{(\ell)}$ is the gradient of the function to be maximized, i.e.,

$$\mathbf{G}_i^{(\ell)} = \nabla C$$

$$= \left[\frac{\partial C}{\partial P_i(\lambda_1)} , \frac{\partial C}{\partial P_i(\lambda_2)} \right] \qquad \text{for the two class case}$$

and $PROJ^{(\ell)}$ is a projection operator that insures that $P_i^{(\ell)}$ is still a probability vector. [Ref. 17]

Based on this technique, the iteration of the initial probabilities $P_i^{(o)}$ is defined as

$$P_i^{(\ell+1)}(\lambda_1) = P_i^{(\ell)}(\lambda_1) + \rho^{(\ell)}\ PROJ^{(\ell)}\ \frac{\partial C}{\partial P_i(\lambda_1)}$$

$$P_i^{(\ell+1)}(\lambda_2) = P_i^{(\ell)}(\lambda_2) + \rho^{(\ell)}\ PROJ^{(\ell)}\ \frac{\partial C}{\partial P_i(\lambda_2)} \qquad (3.18)$$

where $\rho^{(\ell)}$ is a step size which will be developed later.

A method discussed by J. B. Rosen which maximizes a function while satisfying a constraint or constraints is called the gradient projection method [Ref. 19]. The constraint for this case is

$$P_i^{(\ell+1)}(\lambda_1) + P_i^{(\ell+1)}(\lambda_2) = 1 \qquad (3.19)$$

and

$$Q_i(\lambda_1) + Q_i(\lambda_2) = 1$$
$$2Q_i(\lambda_1) + 2Q_i(\lambda_2) = 2 \qquad (3.20)$$

but (3.20) is the summation of the components of the gradient of criterion C, (3.11) and (3.16),

$$\frac{\partial C}{\partial P_i(\lambda_1)} + \frac{\partial C}{\partial P_i(\lambda_2)} = 2 \qquad (3.21)$$

The projection of the gradient at point $\mathbf{P}_i$ on the closed convex region, i.e., the constraint (3.19), is defined as

$$\text{PROJ}^*\mathbf{G}_i = \mathbf{G}_i - \frac{1}{L} \sum_{k=1}^{L} (G_k \mathbf{v}) \tag{3.22}$$

where PROJ is the projection operator, L is the number of classes, $\mathbf{G}$ is the gradient vector, $[G_1, G_2, \ldots, G_2]$, and $\mathbf{v}$ is $[1,1,\ldots,1]$. [Ref. 14] This is shown graphically in Figure 3.3. For the two class case,

$$\mathbf{G}_i = \left[\frac{\partial C}{\partial P_i(\lambda_1)} , \frac{\partial C}{\partial P_i(\lambda_1)} \right] , \quad v = [1,1]$$

and the projection of the gradient (3.22) is a vector with two components. Substituting (3.16) into (3.22), we find

$$\text{PROJ}^{(\ell)} \left[\frac{\partial C}{\partial P_i(\lambda_1)} \right] = 2Q_i(\lambda) - 0.5 \left[\frac{\partial C}{\partial P_i(\lambda_1)} + \frac{\partial C}{\partial P_i(\lambda_2)} \right]$$

$$\text{PROJ}^{(\ell)} \left[\frac{\partial C}{\partial P_i(\lambda_2)} \right] = 2Q_i(\lambda) - 0.5 \left[\frac{\partial C}{\partial P_i(\lambda_2)} + \frac{\partial C}{\partial P_i(\lambda_2)} \right] \tag{3.23}$$

During each iteration, the step size $\rho_i^{(\ell)}$ is normally kept constant and is the largest possible value such that after each iteration, the probabilities, $\mathbf{P}_i$'s, remain within the constraint of $P_i(\lambda_1) + P_i(\lambda_2) = 1, P_i(\lambda_k) > 0.0$, $k = 1,2$ for all i.

However, for the two class case, the step size can be computed for each pixel. Changing the step size each time will provide for a faster convergence rate to the maximum criterion. Examples of this convergence will be shown later.

The maximum value of the step size, $\rho^{(\ell)}$ is found by maximizing the $(\ell+1)$ iteration of (3.24a) and (3.24b), i.e., set $P_i^{(\ell+1)}(\lambda_1) = 1$ and $P_i^{(\ell+1)}(\lambda_2) = 1$, respectively. This will produce two values for the step size,

$$1 = P_i^{(\ell)}(\lambda_1) + \rho_i^{(\ell)}(2Q_i(\lambda_1) - 1)$$

$$1 - P_i^{(\ell)}(\lambda_1) = \rho_i^{(\ell)}(2Q_i(\lambda_1) - 1)$$

$$\rho_i^{(\ell)} = \frac{1 - P_i^{(\ell)}(\lambda_1)}{2Q_i(\lambda_1) - 1}$$

and,

$$1 = P_i^{(\ell)}(\lambda_2) + \rho_i^{(\ell)}(2Q_i(\lambda_2) - 1)$$

$$\rho_i^{(\ell)} = \frac{1 - P_i^{(\ell)}(\lambda_2)}{2Q_i(\lambda_2) - 1}$$

Substituting (3.19) and (3.20) to get

$$\rho_i^{(\ell)} = \frac{P_i^{(\ell)}(\lambda_1)}{1 - 2Q_i(\lambda_1)}$$

The step size must be positive, therefore,

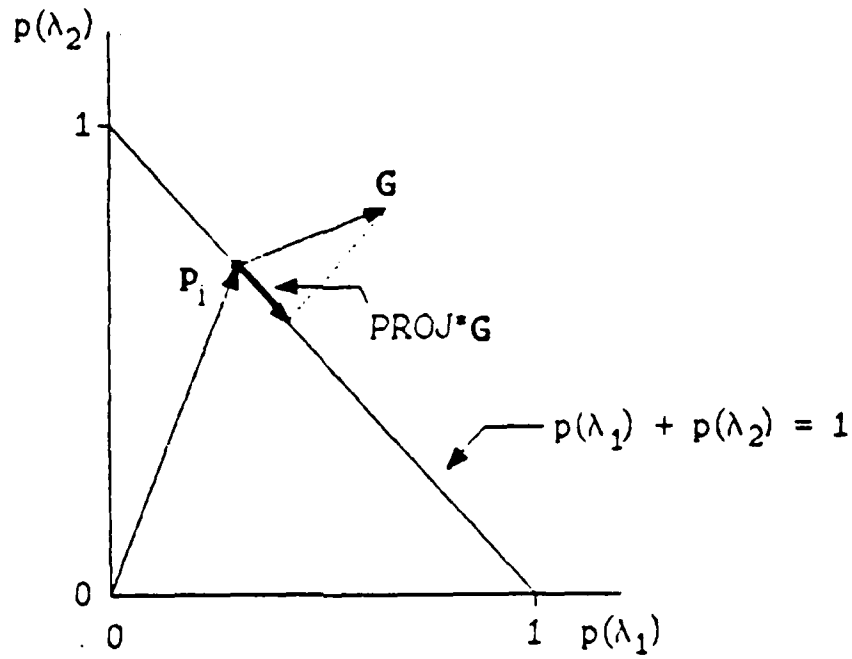

Figure 3.3: Projection of the Gradient, G, on the constraint

$$\rho_i^{(\ell)} = \begin{cases} \dfrac{1 - P_i^{(\ell)}(\lambda_1)}{2Q_i(\lambda_1) - 1}, & \text{if } Q_i(\lambda_i) > 0.5 \\ \dfrac{P_i^{(\ell)}(\lambda_1)}{1 - 2Q_i(\lambda_1)}, & \text{if } Q_i(\lambda_i) < 0.5 \end{cases} \qquad (3.25)$$

In the algorithm which was used in this thesis, both the rate of convergence to the criterion and the number of pixels assigned to each class was controlled by setting the step size to the following values,

$$\rho_i(\ell) = \begin{cases} \alpha_1 \rho_{imax}^{(\ell)}, & \text{if } Q_i(\lambda_1) > 0.5 \\ \alpha 2 \rho_{imax}^{(\ell)}, & \text{if } Q_i(\lambda_2) < 0.5 \end{cases} \qquad (3.26)$$

where α_1 and α_2 are constants whose values are less than cone. The values of α_1 and α_2 are weighting factors which will bias an image to a class, λ_1 or λ_2, and will influence the convergence rate of the criterion.

Figures 3.4(a to c) show the change in the criterion as the number or iterations increases for a cell image which was studied in the noted reference. Each figure represents the three cases, $\alpha_1 = \alpha_2$, $\alpha_1 < \alpha_2$, and $\alpha_1 > \alpha_2$, with the parameter FACT = 1.0 in all cases. These figures show that by increasing the weighting factors, the rate of convergence will increase and these factors, α_1 and α_2, will also control where the criterion will converge. Thus, the control of the relaxation process can be done. The

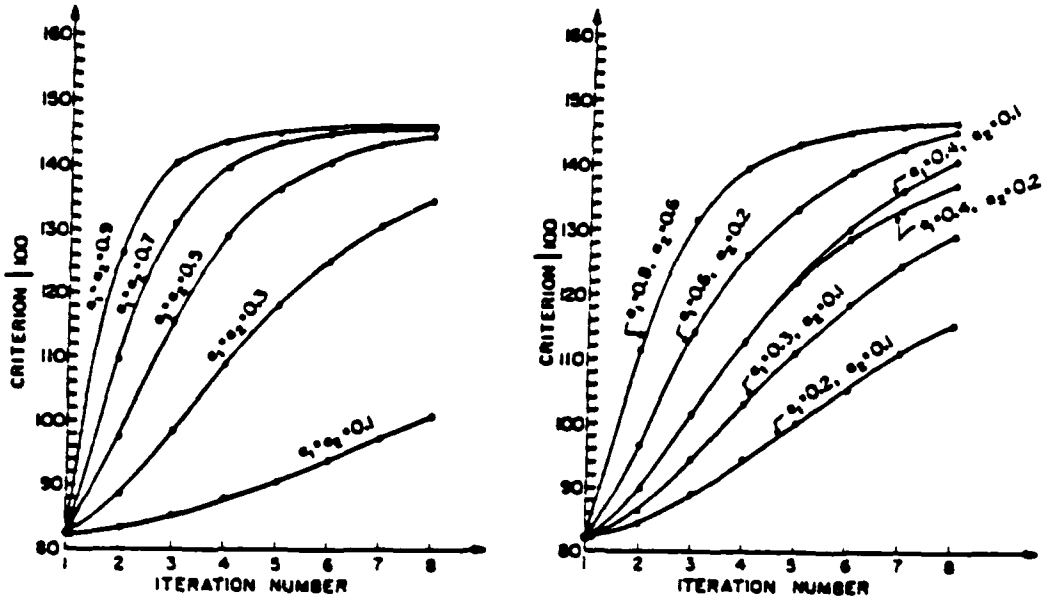

(a) $\alpha_1 = \alpha_2$ (b) $\alpha_1 > \alpha_2$

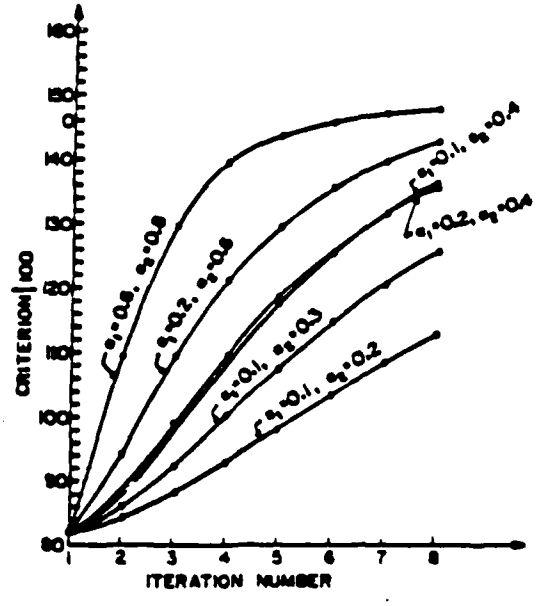

(c) $\alpha_1 < \alpha_2$

Figure 3.4: Variations of the criterion, C, with the iteration number for various values of Alphal and Alpha2 [Ref. 20]

an image at each iteration. Smoothing is defined as the elimination of a small region or regions of one class within a much larger region of the opposite class. As the magnitude of each factor, α_1 and α_2 increases, the smoothing effect decreases. This will be demonstrated in the next chapter. Also, the ratio of α_1 and α_2 controls the bias of a class. Earlier, the parameter FACT was set equal to one. The reason for this is shown in Figure 3.5. The effect of this parameter on the value of the criterion and the convergence rate of the criterion is seen to be minimal [Refs. 15, 20]

A major capability of this process is to automatically select a threshold value. This is a key task in region segmentation. It is important in image processing to select an adequate threshold for extracting objects from their background. In the ideal case, the histogram will have a deep and sharp valley between two peaks representing the object and the background. In a real picture, however, it is sometimes difficult to detect the valley bottom, especially when the valley is flat and broad, imbued with noise, or when the peaks have extremely unequal heights producing no discernible valley. [Ref. 21] In the case where the histogram has a flat and broad valley, a threshold selected too low creates an object (target) which maybe larger than it actually is, or if the threshold is selected

too large, most of the actual target maybe segmented into the background.

In the next chapter, it will be shown that as the number of iterations increases, the peaks in the histogram will move farther apart, and the average brightness will increase. When the peaks are far apart, the mean value of the original image or the segmented image can be used as the threshold value. [Ref. 15] This is why the gradient relaxation is advantageous as compared to other methods in segmenting infrared images.

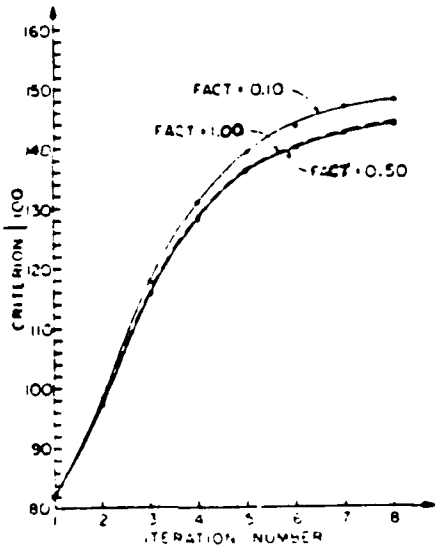

Figure 3.5: Variation of the criterion, C with the iteration number for 3 values of FACT [Ref. 14]

IV. ANALYSIS OF IMAGES

A. IMAGES UNDER ANALYSIS

The gradient relaxation segmentation method discussed in the previous chapter was demonstrated on several infrared images. Ten images were used to evaluate the performance of this segmentation technique. The first image is a still photo of a ship with low contrast (poor visibility), see Figure 4.1(a). The other nine images were obtained from an uncooled focal plane infrared sensor (Figures 4.1(b) - (j)). The sensor was placed on a platform on which the sensor was rotated to simulate the situation of a rotating missile. This is why the targets are seen at different viewing angles. The images were recorded on video disc. Using the EYECOM digitizer, individual frames were extracted from the video disk. The video disc contained approximately 20 minutes of video data of several ships in various contrasts. The scenes contained a wide variation of noise within the images. Instead of attempting to analyze all of the frames (approximately 64,000 frames), it was decided to select images which were representative of most of the frames and situations depicted on the video disc. The purpose is to determine how effective the relaxation segmentation method is for these images.

Figure 4.1(a): A ship with low contrast.

Three criteria were used in the selection of the images:

1. Find images where the target stands out from the background and is not degraded significantly by noise. The images which met this criteria are Figures 4.1(a), (c), and (d).
2. Find target near or within part or all of the background noise with an intensity level near the intensity level of the target. This is seen in Figures 4.1(b), (e), (f), and (g).
3. Collect a series of frames as the target is rotating, showing how the noise changes from frame to frame. The series selected includes targets near noise of similar intensity (see Figures 4.1(g), (i), and (j)). It also includes a target which because of the noise is fragmented into several objects, to the point where the target itself appears to be background noise (see

Figure 4.1(b): A medium-size ship

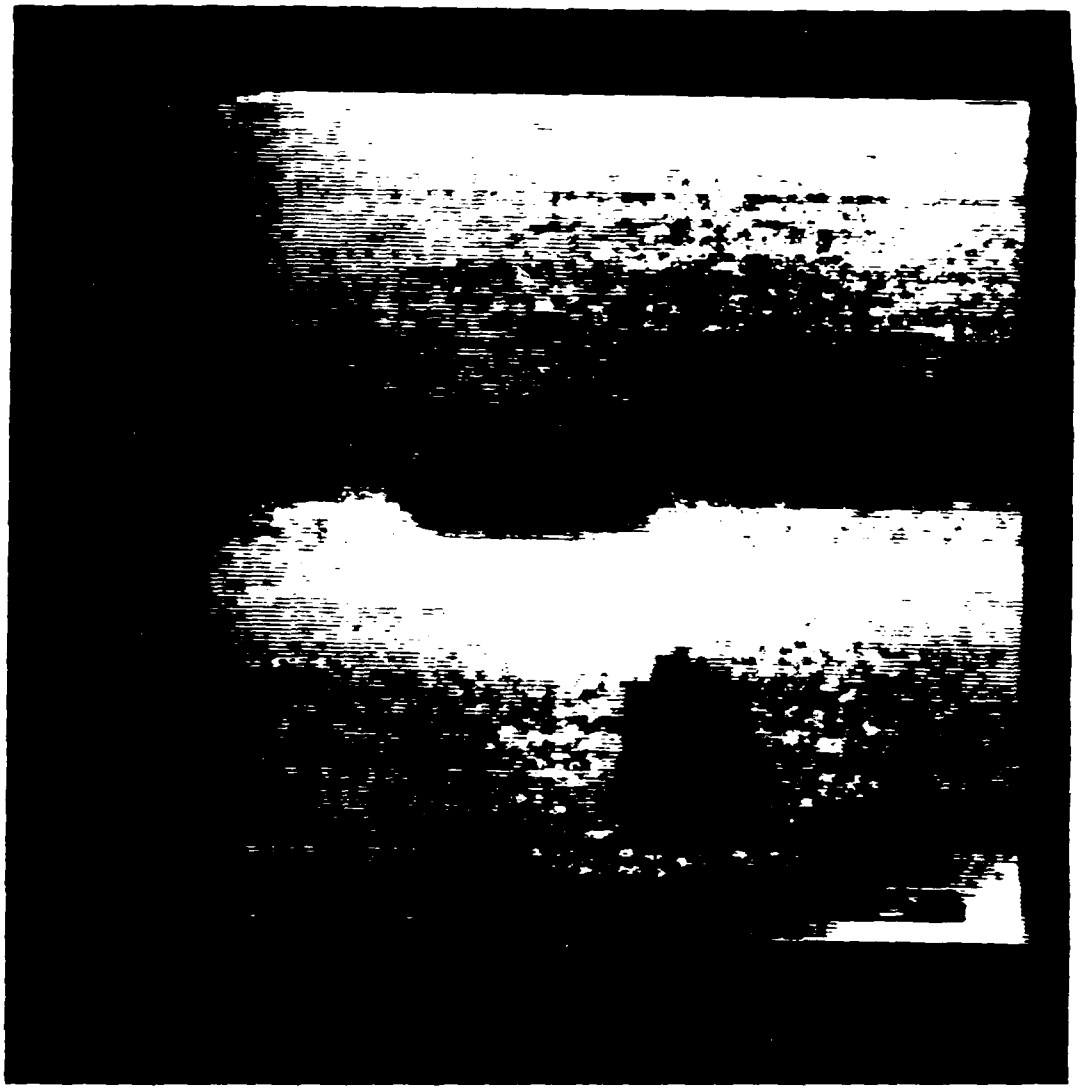

Figure 4.1(c) A sailboat

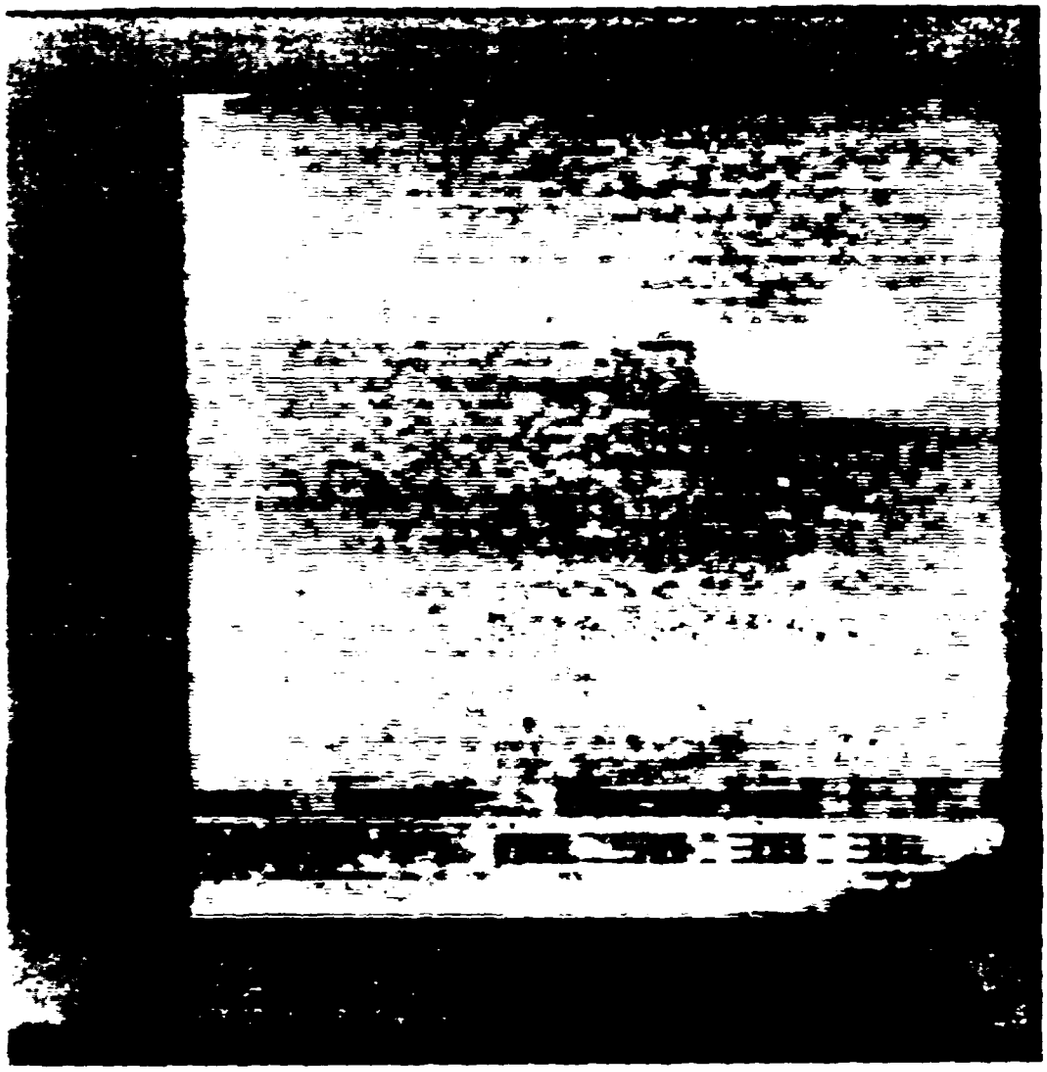

Figure 4.1(d): A large ship

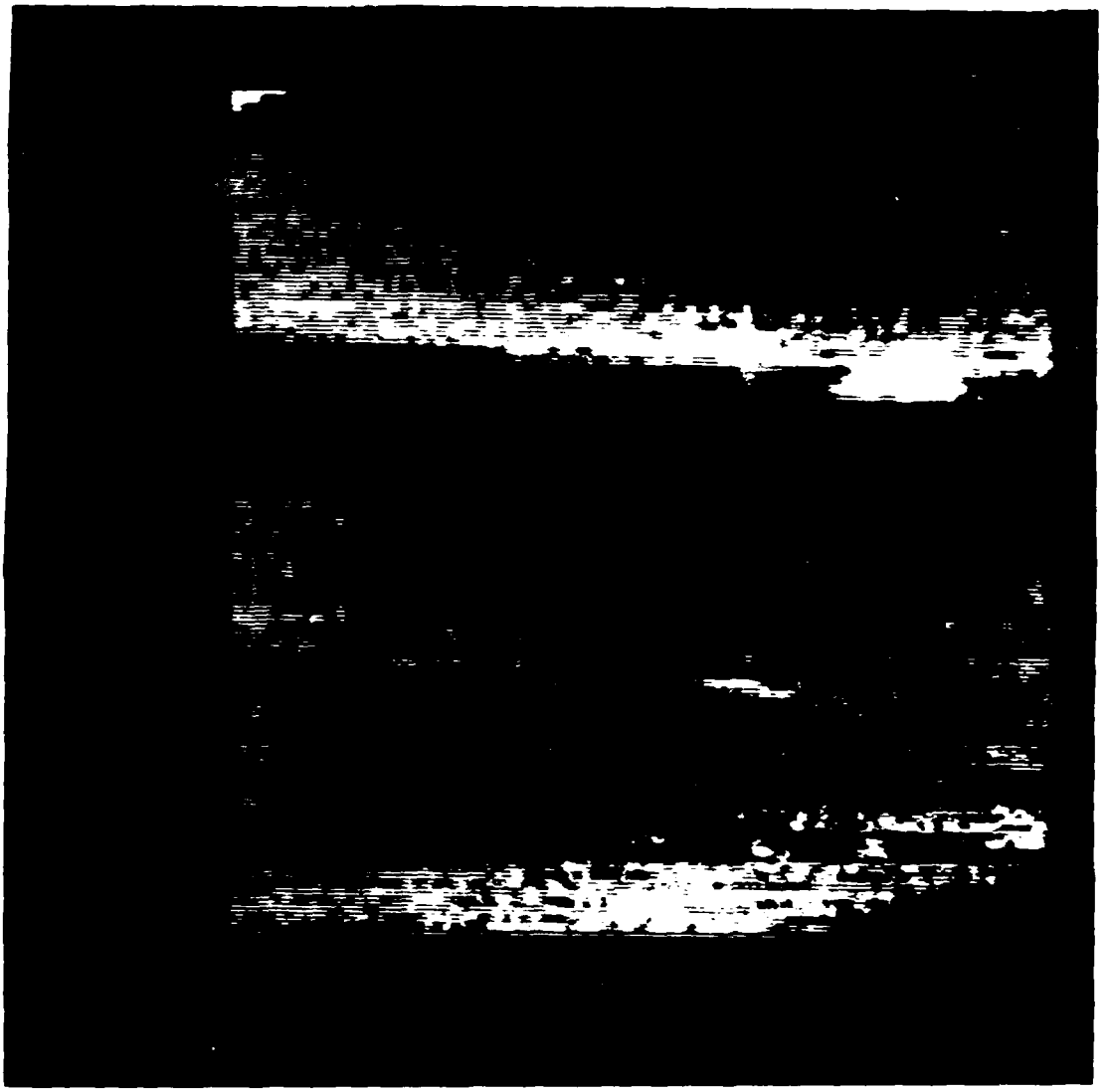

Figure 4.1(e): First in a series of six images (Ship A)

Figure 4.1(f): Second in a series of six images (Ship B)

Figure 4.1(g): Third in a series of six images (Ship C)

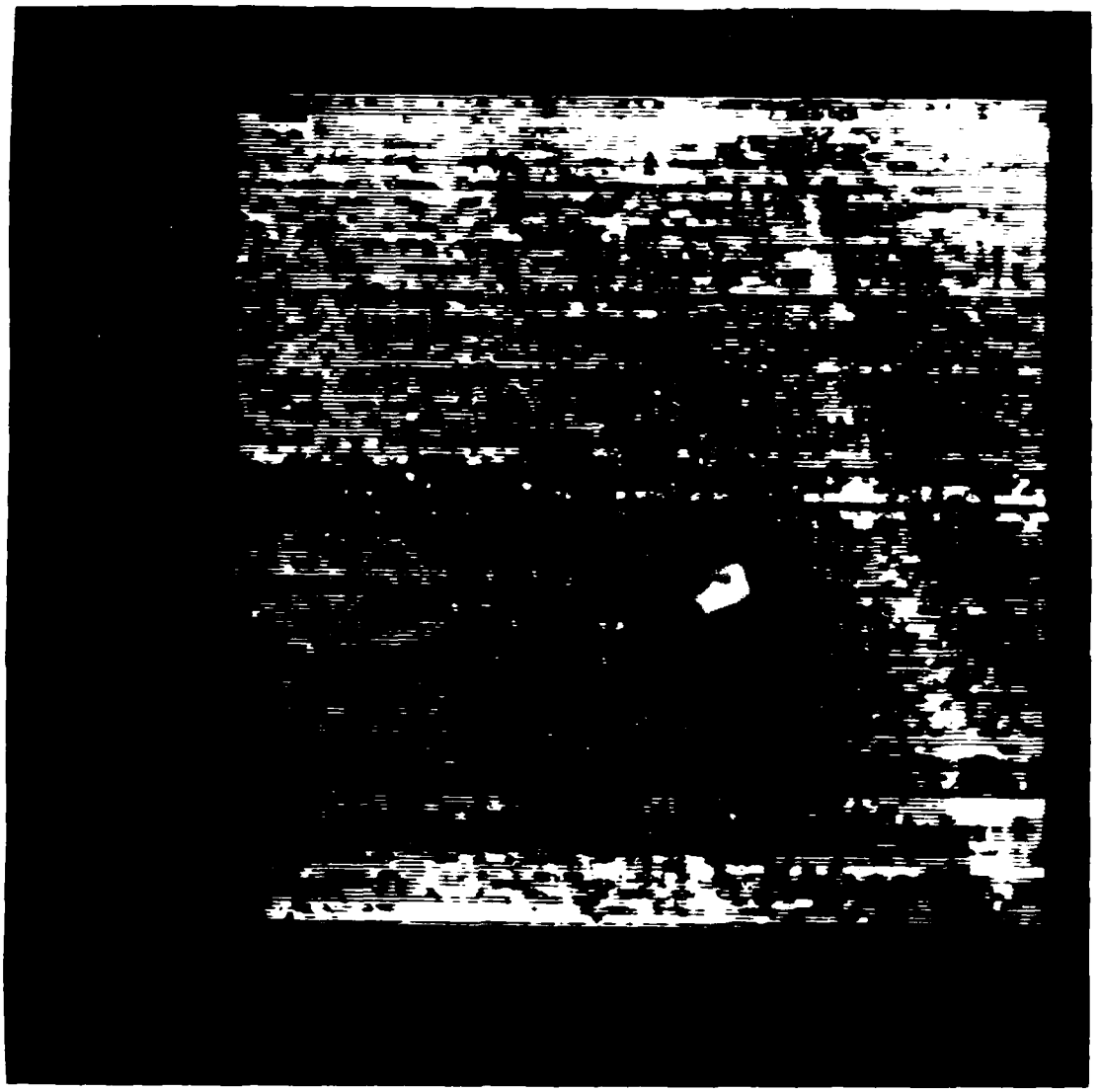

Figure 4.1(h): Fourth in a series of six images (Ship D)

Figure 4.1(i): Fifth in a series of six images (Ship E)

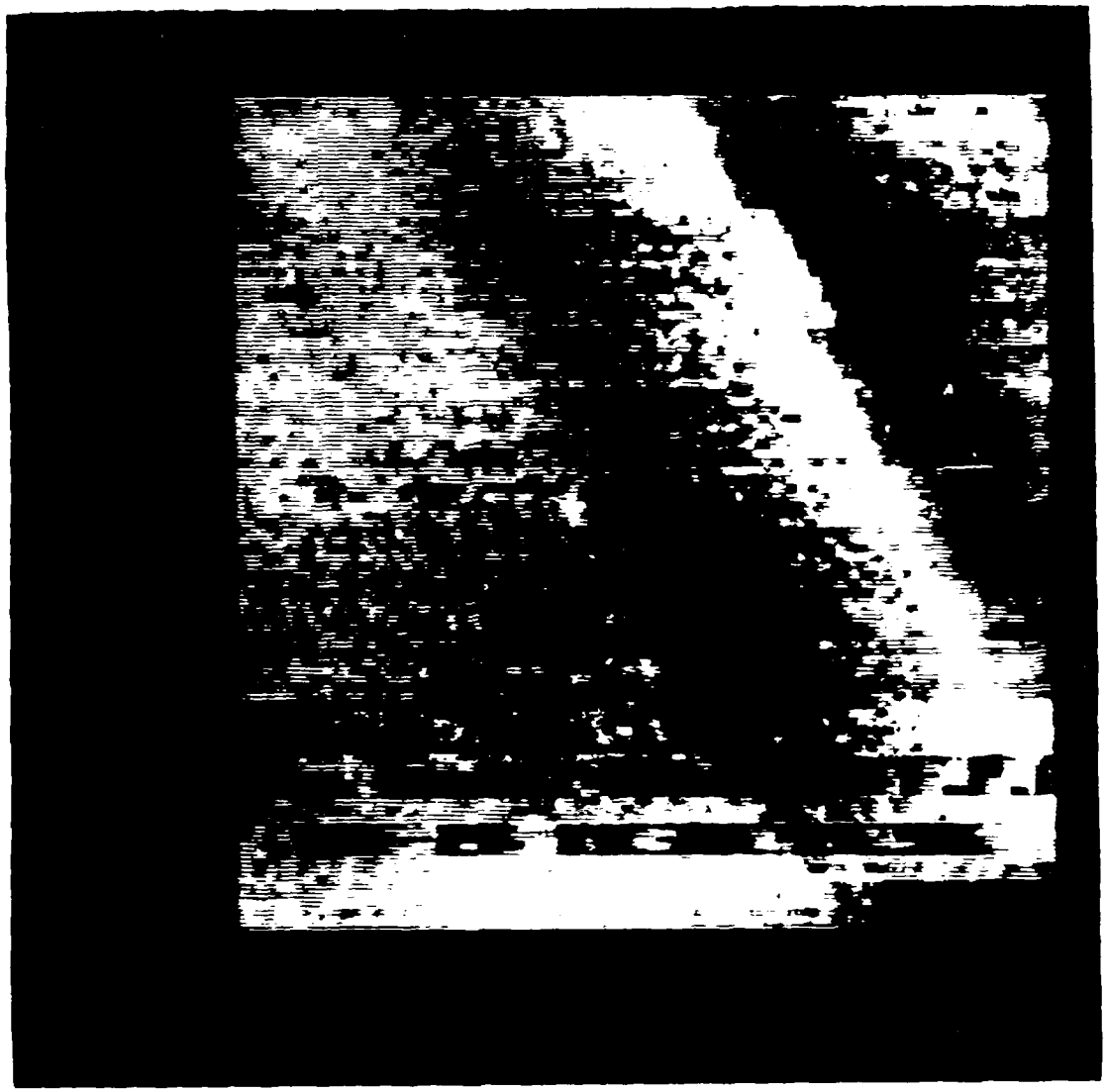

Figure 4.1(j): Sixth in a series of six images (Ship F)

Figure 4.1(h)). The intention is to see if the target can be segmented from the noise background well enough to be able to detect it as a target.

These cases obviously do not account for all situations, but are representative of the noisy infrared images which were available for this study.

The targeted object was then extracted from the original 512 by 512 image to form a smaller 64 by 256 image which requires much less time to process. Figures 4.2(a) - (j) depicts each of these images with their associated histograms.

Noise in the images come from various sources, either natural or the sensor. Noise sources include glare off the surface of the water, atmospheric interference, such as scattering and attenuation of the cloud and haze. Thermal noise is introduced since the sensor is uncooled. Transmission noise was introduced when the image was recorded onto the video disc and when it is digitized using the EYECOM digitizing system.

The COMTAL VISION ONE/20 Image Processing System was used to display the images and to produce the associated histogram. COMTAL VISION ONE/20 is a complete image processing system with built-in interactive processing and control capabilities. The system produces high spatial resolution video images over a range of 256 gray levels.

(a) Ship with low contrast

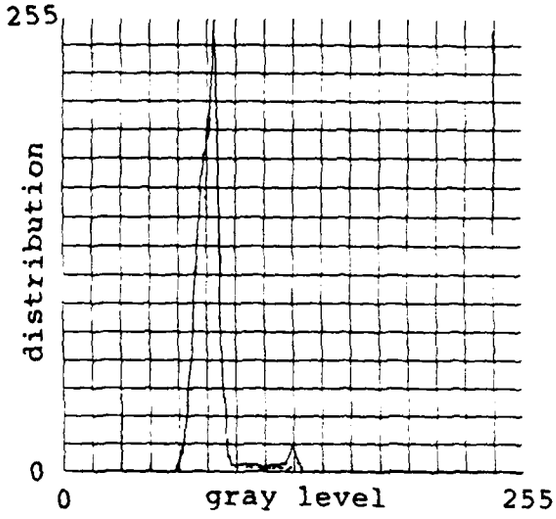

(b) Medium-size ship from Figure 4.1(b)

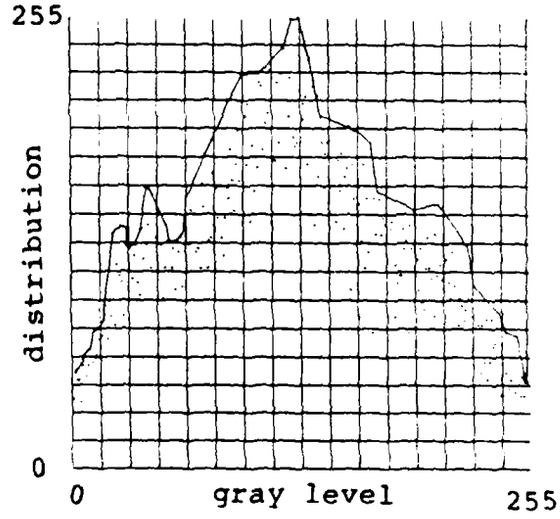

Figure 4.2: Original 64 X 256 images extracted from Figure 4.1 images with their gray-level histogram

(c) Sailboat from Figure 4.1(c)

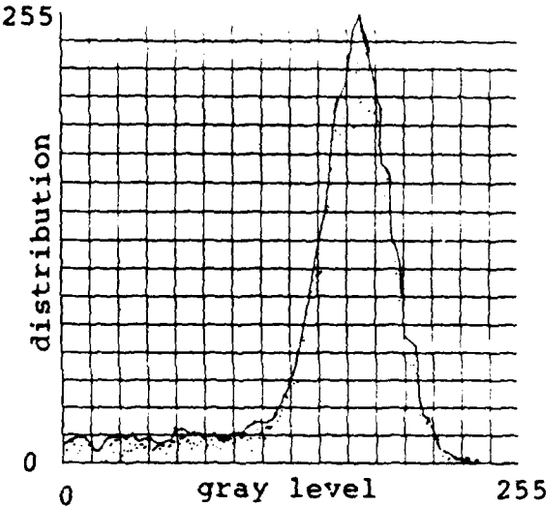

(d) Large ship from Figure 4.1(d)

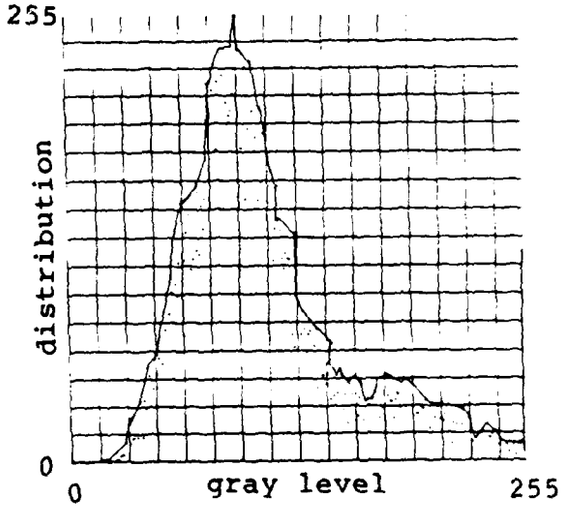

(Figure 4.2 continued)

(e) Ship A from Figure 4.1(e)

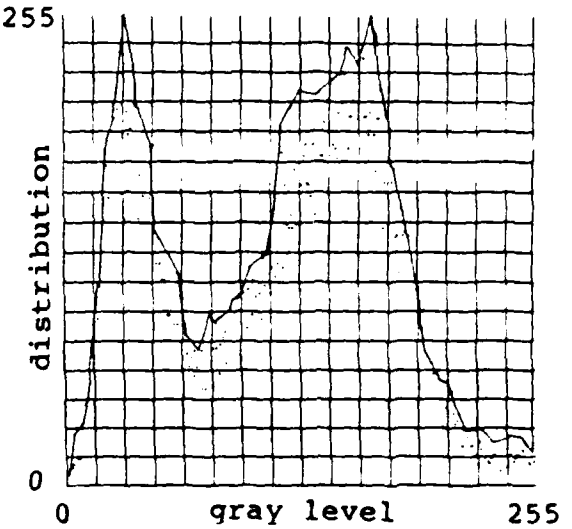

(f) Ship B from Figure 4.1(f)

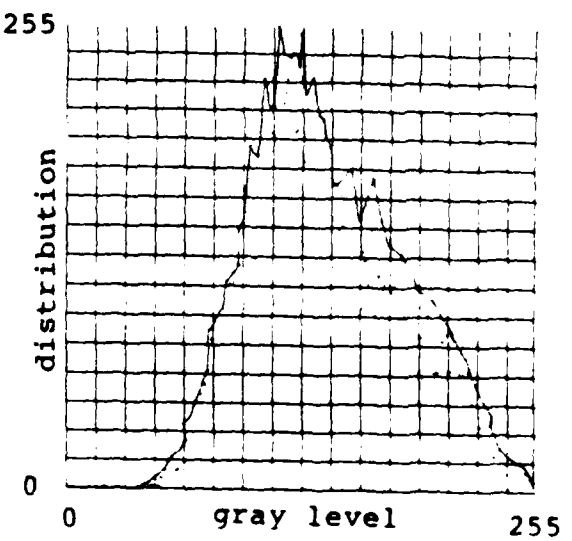

(Figure 4.2 continued)

(g) Ship C from Figure 4.1(g)

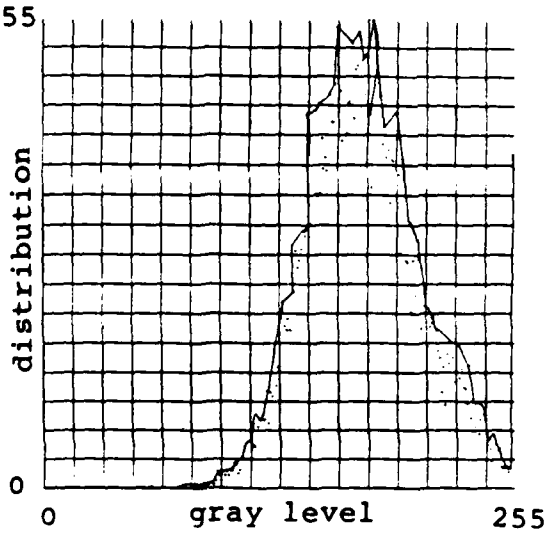

(h) Ship D from Figure 4.1(h)

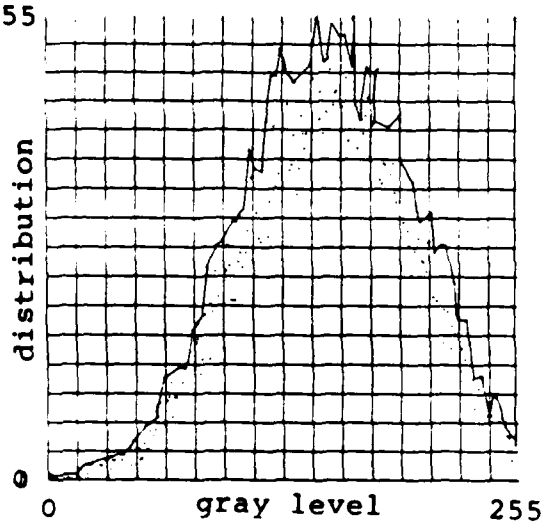

(Figure 4.2 continued)

(i) Ship E from Figure 4.1(i)

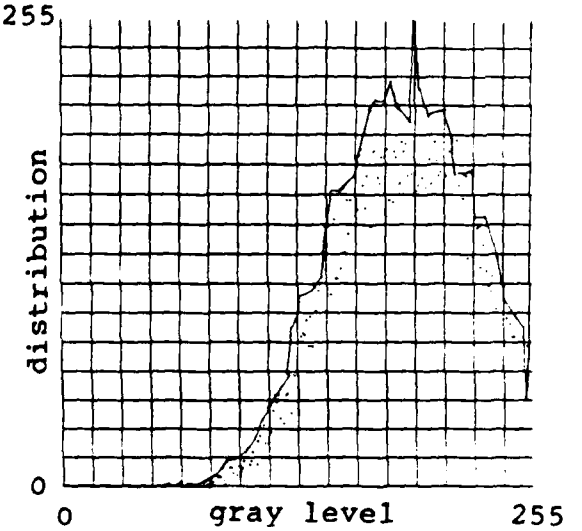

(j) Ship F from Figure 4.1(j)

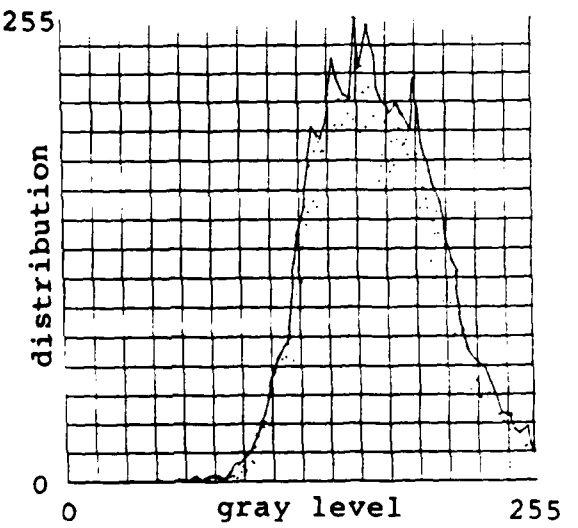

(Figure 4.2 continued)

The distribution of the pixels over the gray level range is completed by the COMTAL processor in the following manner. The processor counts all occurrences of each gray level in the image. This count (the total number of pixels at each gray level) is divided by the highest count and then multiplied by 256. This number is subtracted by 1 to yield the distribution of that gray level in the figures. The highest normalized count is always 255. [Ref. 22]

The points in the original histograms were not connected. To provide a better feeling for the shape of the histogram, it was decided to connect those points which presented a general outline of the gray level distribution. The points selected are generally the highest point in a selected neighboring group of points.

The histograms of each of these images generally shows the distribution between the background and the target. In Figures 4.2(a) and (e) - (j), it is possible to see a separation between the peak background level and the peak target level. However, in each of these cases it would be difficult to select a threshold value which could be used to perform an effective segmentation as discussed in Chapter II. By using the gradient relaxation technique, the problem of determining a critical threshold value is easy.

The selection of the weighing factors, Alphal and Alpha2, and the number of iterations necessary to perform

the segmentation is very important, as mentioned in the previous chapter. The selection of these parameters is influenced by the detected size of the segmented target, the needed accuracy of the object outline, and separation of the gray level peaks. It also determines how quickly the histogram of the segmented image reaches its widest separation of the gray peak levels. This was also demonstrated in the last chapter. The following parameters were used in performing the experiments on the segmented images:

Alphal:	The weighing factor on pixels with gray levels greater than the mean.
Alpha2:	The weighing factor on pixels with gray levels less than the mean.
Iter:	The number of iterations of the relaxation routine.
Threshold (THD):	The threshold value is used to determine which pixels will be part of the labeled region. Two values were selected in each image. The first value of 220 was chosen because it is assumed that the higher intensities are part of the target. The second value chosen is the mean gray level intensity of the original image.
Region:	The total number of labeled regions. A labeled region is a grouping of pixels with intensities greater than the threshold, THD.
Area:	The number of pixels in the largest labeled region.
Perimeter:	The number of pixels along the boundary of the largest labeled region.

Shape: This is a measure of the relationship between the area and the perimeter of the largest labeled region. It is equal to

Shape = 2*Area/Perimeter

The shape is small for narrow objects. The shape is large for rounded objects.

B. APPLICATIONS OF THE GRADIENT RELAXATION ROUTINE

The relaxation routine was applied to each of the images shown in Figure 4.2 and are separated into ten separate cases. The criteria used in the analysis is as follows:

1. Are the regions uniform and homogeneous with respect to a gray level?
2. Do the regions contain gaps (holes), and if so, can successive iterations smooth the segmented region?
3. Are the peaks in the histograms more distinct?
4. Does the target conform to a desired shape?
5. Is a target detected?
6. Can the detected object be used in the classification process?

The general format of the experiment entailed applying different values of the values Alphal and Alpha2 to the images for several iterations and to observe the effect on the original images. The values were subjectively chosen to test for the cases when Alphal = Alpha2, Alphal < Alpha2, and Alphal > Alpha2. The maximum number of iterations selected was based on the theoretical results shown in Figure 3.4 (Chapter III). These figures consistently showed that the criterion was saturated after eight or more

iterations. Using more iterations would not have significantly improved the segmentation.

Each case includes a discussion on the effect of the algorithm on that image. A figure of the segmented image and the corresponding histogram are shown. Also included is a table summarizing the change in the area, perimeter, and the shape of the segmented region(s) for the different settings of the weighing factors, threshold, and number of iterations.

1. Ship in Low Contrast (Figure 4.2(a))

The number of iterations is important in determining the peak gray level separation of the background and the target. Figures 4.3(a)-(d) shows how each iteration increases this separation. In the original image, the separation is approximately 45 levels; after on iteration it is almost 135 levels, after four iterations it is almost 225, and after eight iterations, the separation is approximately 250 levels.

Four cases involving different Alphal, Alpha2 parameters and number of iterations were applied to the image of Figure 4.2(a). Results of this application are seen in Figure 4.3 and Table 4.1. These parameters determine the form and gray level intensity of the segmented scene. Setting the value of Alphal $\geq$ Alpha2 increases the apparent size of the target. This is seen in Figures

(a) Alphal = .3
Alpha2 = .3
Iter = 1

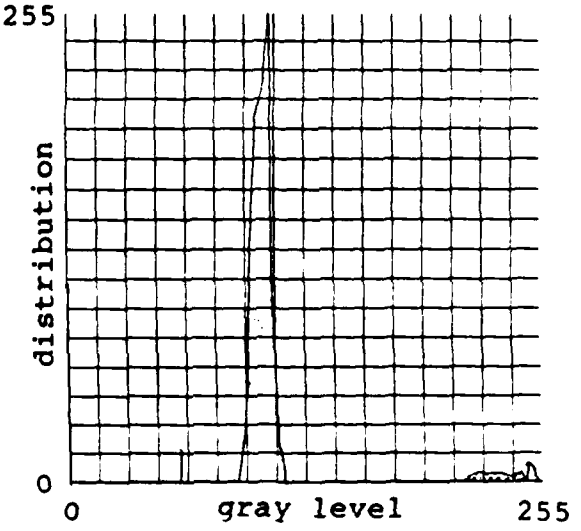

(b) Alphal = .3
Alpha2 = .3
Iter = 2

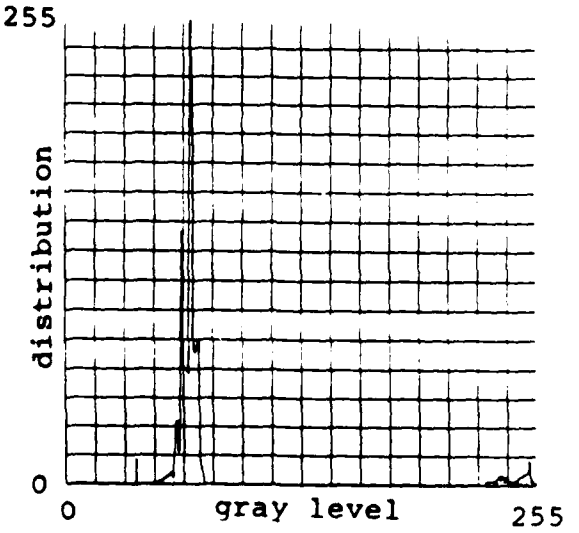

Figure 4.3: Results of relaxation segmentation on ship with low contrast

(c) Alphal = .3
Alpha2 = .3
Iter = 4

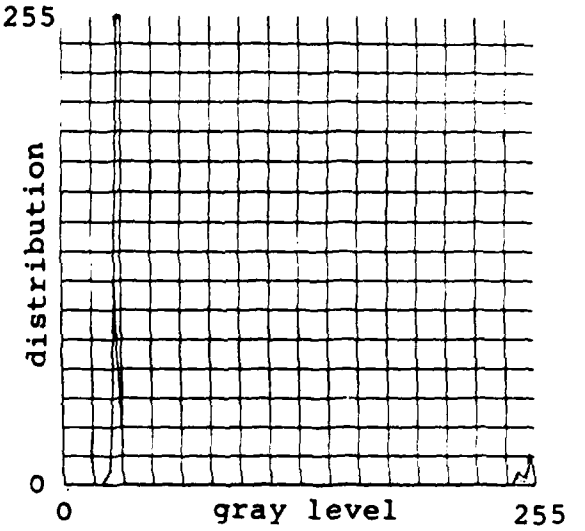

(d) Alphal = .3
Alpha2 = .3
Iter = 8

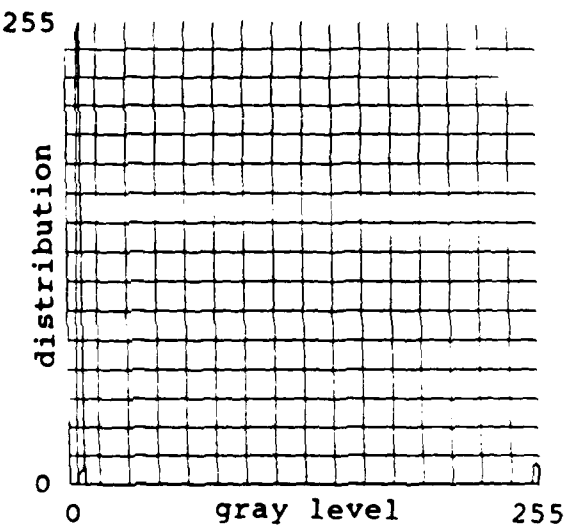

(Figure 4.3 continued)

(e) Alphal = .6
Alpha2 = .2
Iter = 2

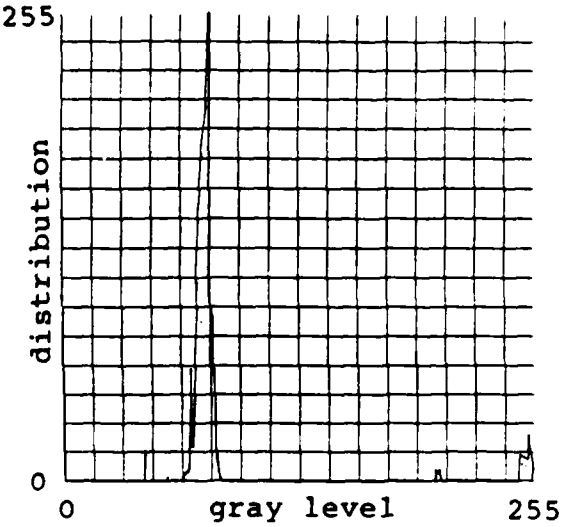

(f) Alphal = .6
Alpha2 = .2
Iter = 8

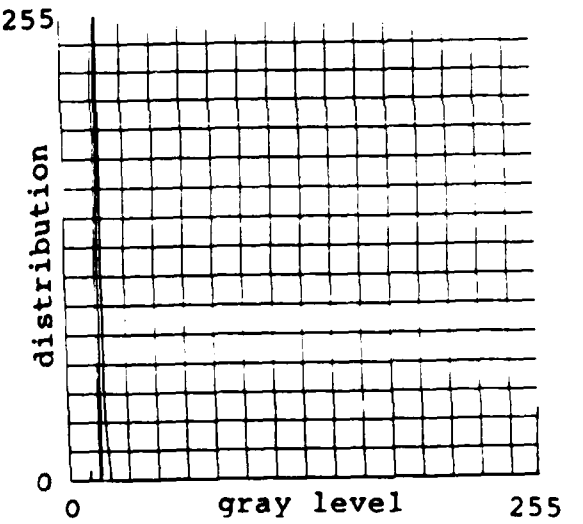

(Figure 4.3 continued)

(g) Alphal = .2
Alpha2 = .6
Iter = 2

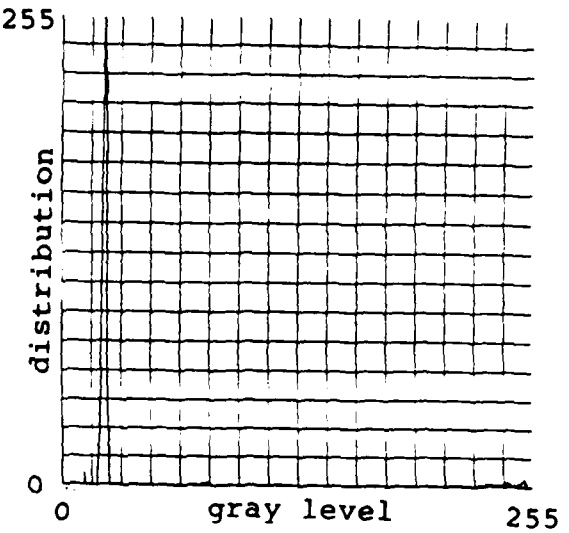

(h) Alphal = .2
Alpha2 = .6
Iter = 8

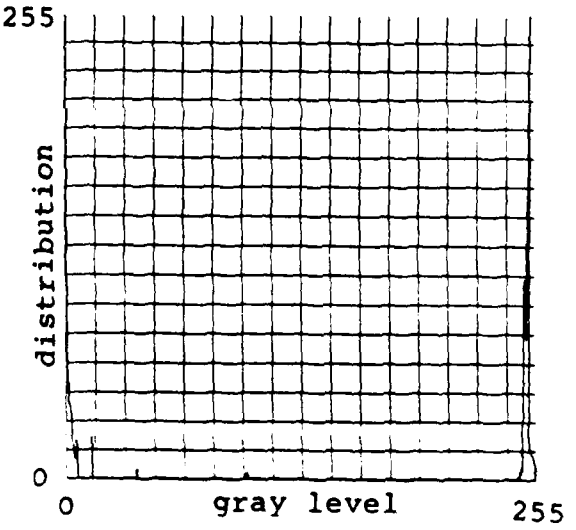

(Figure 4.3 continued)

(i) Alphal = .1
Alpha2 = .4
Iter = 2

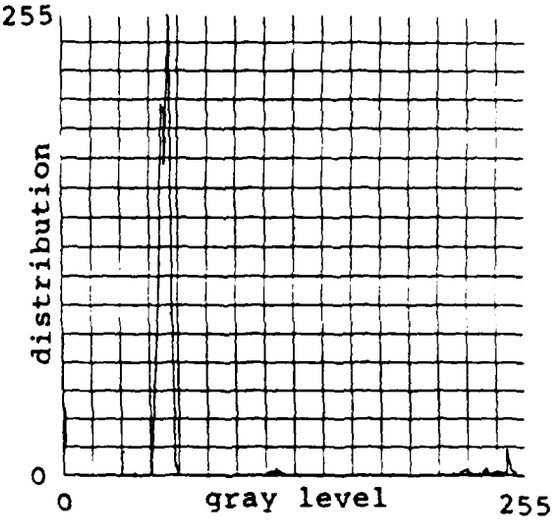

(j) Alphal = .1
Alpha2 = .4
Iter 8

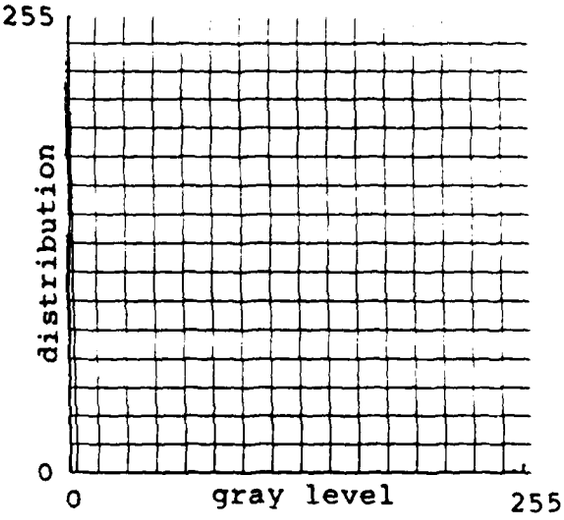

(Figure 4.3 continued)

TABLE 4.1
QUANTITATIVE RESULTS OF SHIP WITH LOW CONTRAST

ALPHA1	ALPHA2	ITER	THD	REGION	AREA	PERIM	SHAPE
0.3	0.3	1	220	1	808	134	12.06
0.3	0.3	1	82	1	15067	607	49.65
0.3	0.3	2	220	1	904	131	13.80
0.3	0.3	2	82	1	913	131	13.94
0.3	0.3	4	220	1	900	131	13.74
0.3	0.3	4	82	1	905	131	13.82
0.3	0.3	8	220	1	896	131	13.68
0.3	0.3	8	82	1	899	131	13.73
0.6	0.2	2	220	1	912	131	13.92
0.6	0.2	2	82	4	1438	219	13.13
0.6	0.2	8	220	1	1222	146	16.74
0.6	0.2	8	82	1	1222	146	16.74
0.2	0.6	2	220	1	720	121	11.90
0.2	0.6	2	82	1	737	127	11.61
0.2	0.6	8	220	1	541	109	9.93
0.2	0.6	8	82	1	547	109	10.04
0.1	0.4	2	220	1	657	120	10.95
0.1	0.4	2	82	1	912	131	13.92
0.1	0.4	8	220	1	467	96	9.73
0.1	0.4	8	82	1	506	102	9.92

MEAN = 82

4.3(a)-(f). The resultant image looks more like a tank, not like a ship. By increasing the number of iterations, the region grows larger as defined by the area. However, in the cases (Figures 4.3(e)-(j)) where Alphal < Alpha2, the segmented region appears to be closer to the true size in the original image, and the region gets smaller as the number of iterations increase. All of the regions in each image are uniform and there are no holes within the regions. The peaks in the histogram are widely separated and

distinct. Results in the table shown that the shape becomes more clearly defined with more iterations. The table also shows that the mean is a reasonable value to use as a threshold. It is evident from the result that this type of scene does allow the relaxation routine to detect a target and would allow for the possible classification of the target if the proper weighing factors are selected.

2. Medium-size Ship (Figure 4.2(b))

Results of this experiment are seen in Figure 4.4 and Table 4.2. This is an image which clearly shows the effect of the number of iterations imposed on establishing well defined peaks. Figures 4.4(g)-(j) display the effects on the same image with one, two, four, and eight iterations. After one iteration, a valley between the peaks is better defined than the original histogram, and after eight iterations the separation is near a maximum.

The weighing factors have a tremendous affect on the segmented regions. Figures 4.4(a)-(d) show that if Alphal $\geq$ Alpha2 the region increases in area and the target cannot be detected. In the case where Alphal < Alpha2 the target is detectable. By increasing the number of iterations, the segmented region develops into a form which can be neither detected as a ship nor classified as a ship as was seen in the result of the first case. Fewer iterations also produce more segmented regions (Table 4.2) which are small.

TABLE 4.2
QUANTITATIVE RESULTS OF MEDIUM-SIZE SHIP

ALPHA1	ALPHA2	ITER	THD	REGION	AREA	PERIM	SHAPE
0.3	0.3	2	220	2	1428	403	7.09
0.3	0.3	2	128	2	1428	403	7.09
0.3	0.3	8	220	3	4025	668	12.05
0.3	0.3	8	128	2	4109	732	11.23
0.6	0.2	2	220	4	2209	344	12.84
0.6	0.2	2	128	3	2512	475	10.57
0.6	0.2	8	220	5	5584	1075	10.87
0.6	0.2	8	128	5	5605	1024	10.95
0.2	0.6	2	220	4	1154	376	6.14
0.2	0.6	2	128	3	2883	513	11.24
0.2	0.6	8	220	1	2643	587	9.01
0.2	0.6	8	128	1	2663	553	9.63
0.1	0.2	1	220	1	851	338	5.04
0.1	0.2	1	128	2	988	289	6.84
0.1	0.2	2	220	3	968	396	4.89
0.1	0.2	2	128	2	2732	523	10.45
0.1	0.4	4	220	4	1089	404	5.39
0.1	0.4	4	128	1	2684	561	9.57
0.1	0.4	8	220	2	1437	419	6.86
0.1	0.4	8	128	2	2133	492	8.67

MEAN = 128

But, increasing the number of iterations there are fewer regions resulting and these regions are larger. With more iterations, the region becomes more homogeneous, but still contains gaps. The example of when Alphal > Alpha2, demonstrates how noise near the target becomes part of the target. This is because the Alphal weights the higher intensity, thus causing the growth. This is a good choice of why Alphal < Alpha2 is chosen. It confines the higher

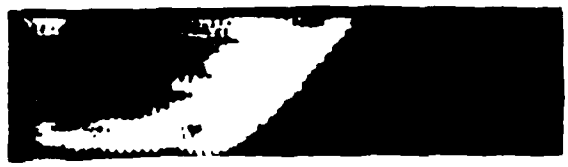

(a) Alphal = .3
Alpha2 = .3
Iter = 2

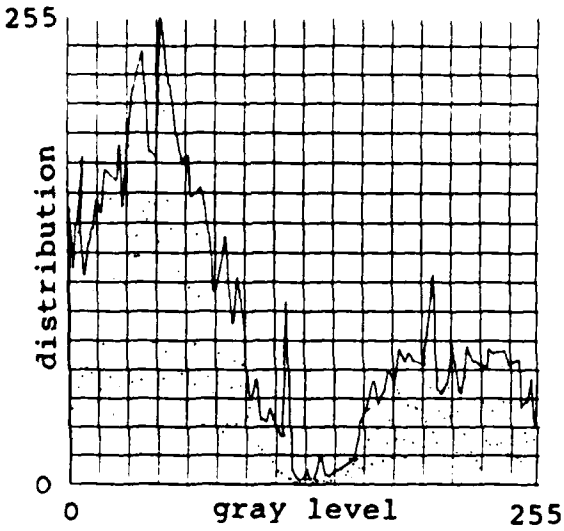

(b) Alphal = .3
Alpha2 = .3
Iter = 8

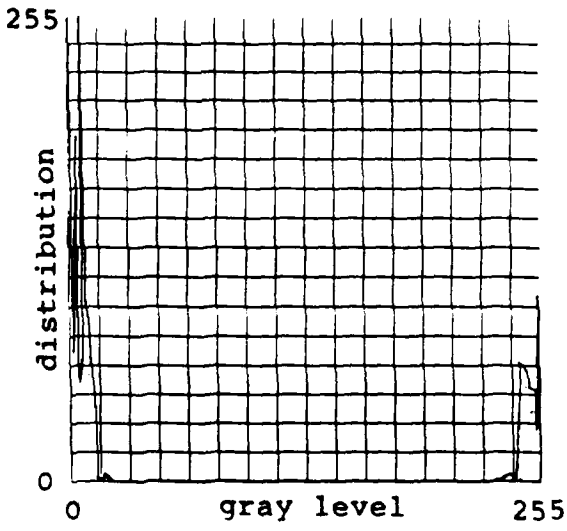

Figure 4.4: Result of relaxation segmentation on medium-size ship

(c) Alphal = .6
Alpha2 = .2
Iter = 2

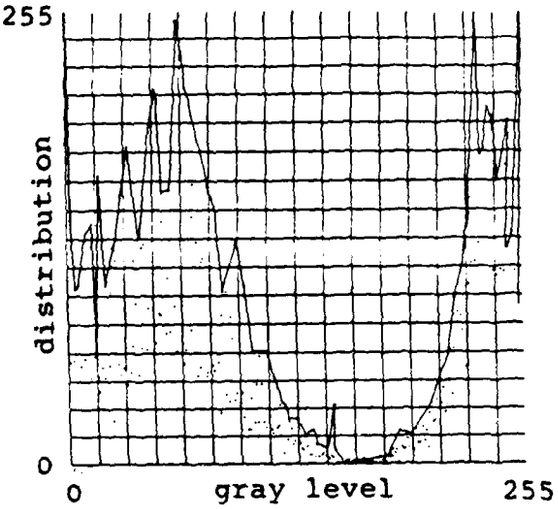

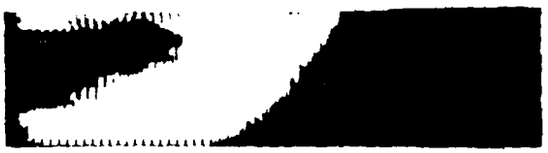

(d) Alphal = .6
Alpha2 = .2
Iter = 8

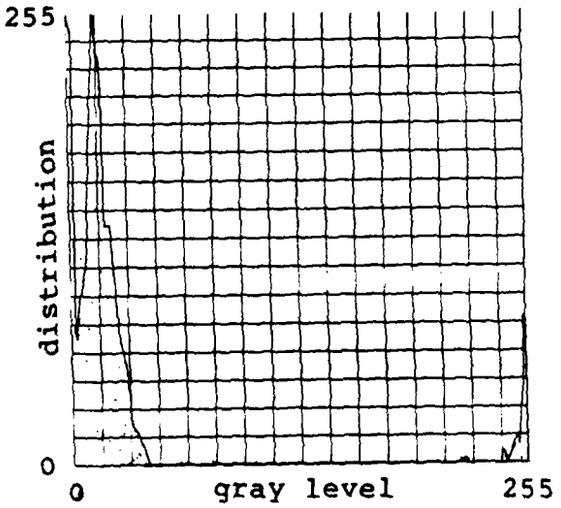

(Figure 4.4 continued)

(e) Alphal = .2
Alpha2 = .6
Iter = 2

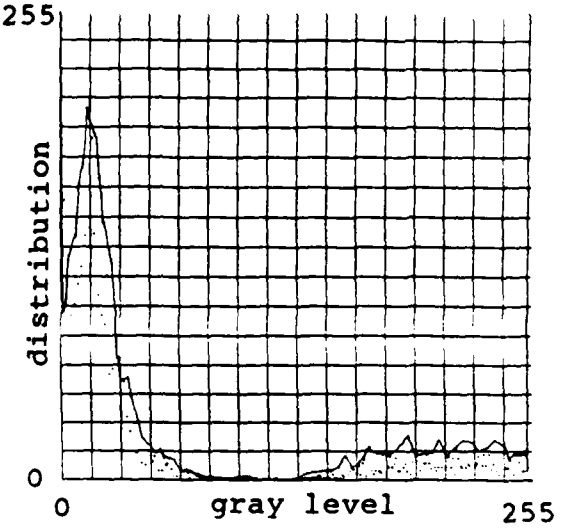

(f) Alphal = .2
Alpha2 = .6
Iter = 8

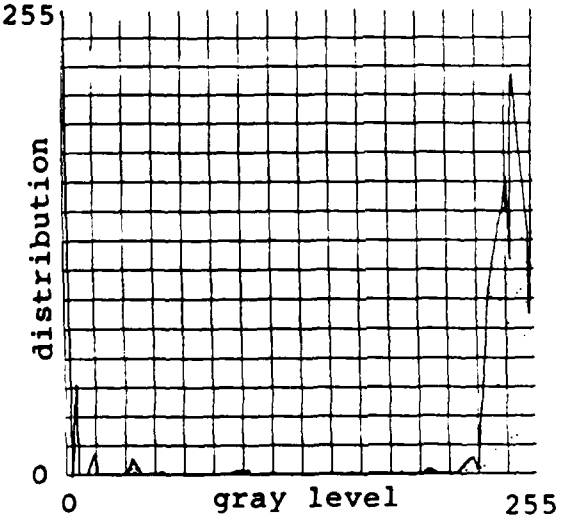

(Figure 4.4 continued)

(g) Alpha1 = .1
Alpha2 = .4
Iter = 1

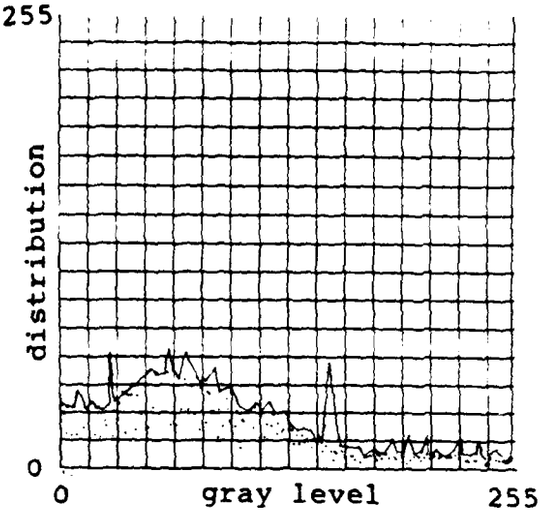

(h) Alpha1 = .1
Alpha2 = .4
Iter = 2

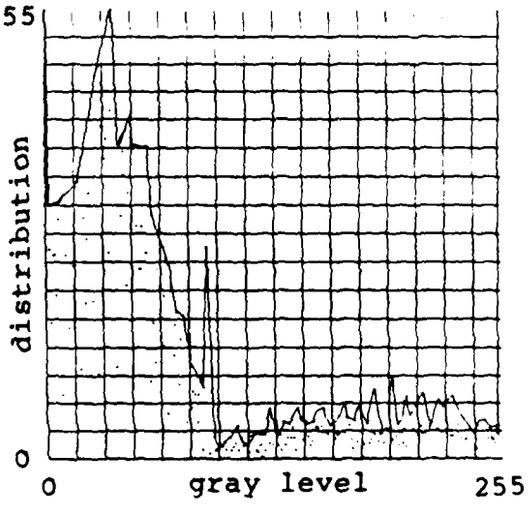

(Figure 4.4 continued)

(i) Alphal = .1
Alpha2 = .4
Iter = 4

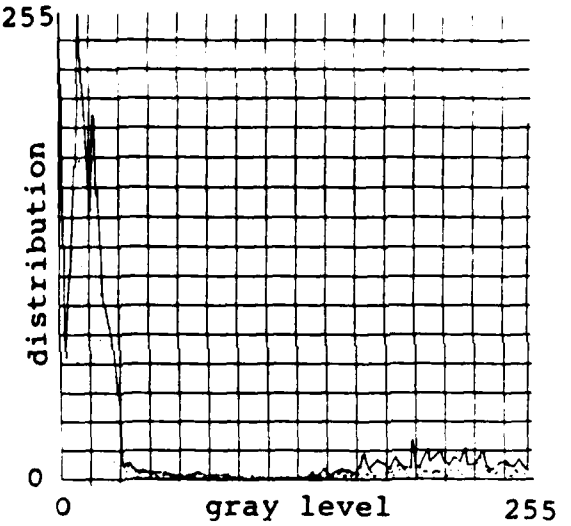

(j) Alphal = .1
Alpha2 = .4
Iter = 8

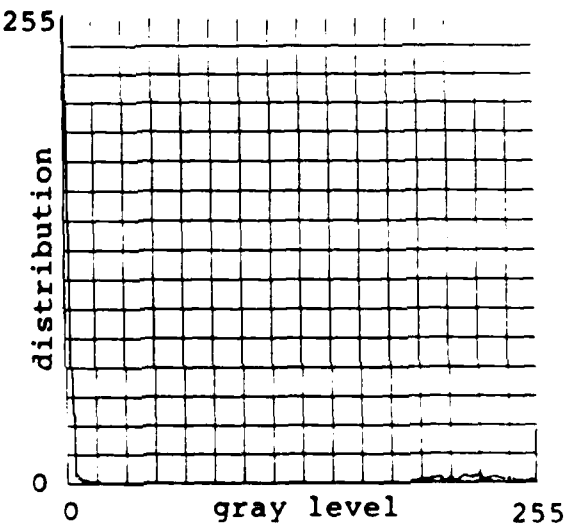

(Figure 4.4 continued)

gray level intensities to the target and separates it from the adjacent noise.

3. Sailboat (Figure 4.2(c))

The image is a black hot inverted infrared image. For the relaxation routine to work properly, the object to be segmented must be lighter than the background. Therefore, the image must be inverted first. Figures 4.5(a)-(d) show results of segmenting this image. This image is similar to the first case (ship of low contrast) in that it provides for a detectable target and as seen in Figures 4.5(c)-(d), it could be classified as a sailboat. This is more readily observed in Figure 4.5(c). This case shows that increasing the number of iterations does not necessarily decrease the size of the region as was seen in earlier cases (Table 4.3). The images are uniform and homogeneous and contain no holes; peaks are distinct, sharp, and widely separated.

4. Large Ship (Figure 4.2(d))

This image is a good example of an object in a noisy background which can be segmented into an image which is both detectable and can be classified. Figures 4.6(a)-(d) depict the effect of relaxation on this image. The best results are seen in Figures 4.6(a) and (b) where the gray level peaks are clearly defined and widely separable. These

(a) Alphal = .6
Alpha2 = .2
Iter = 2

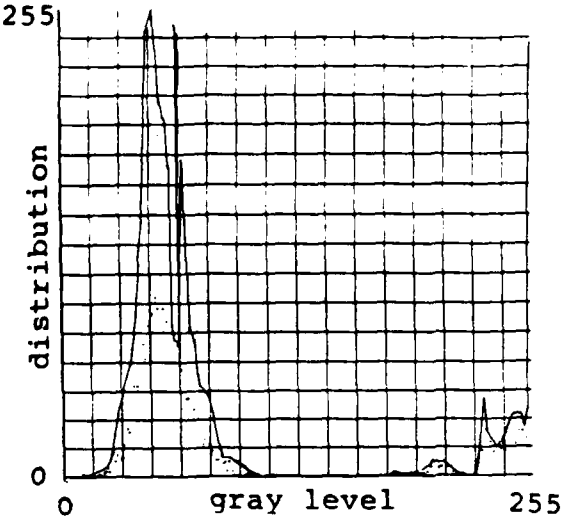

(b) Alphal = .6
Alpha2 = .2
Iter = 8

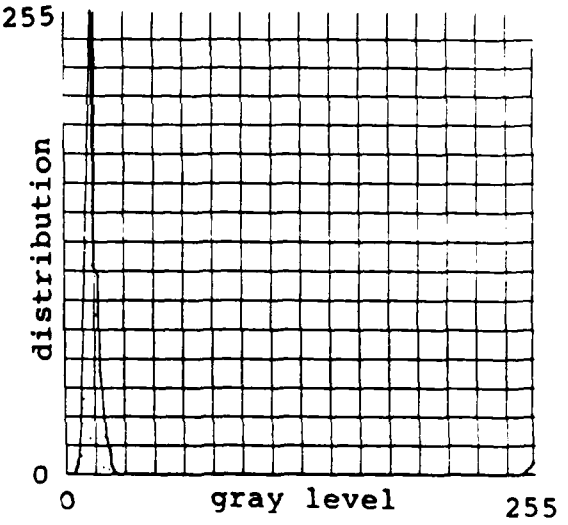

Figure 4.5: Results of relaxation segmentation on a sailboat

(c) Alphal = .1
Alpha2 = .4
Iter = 2

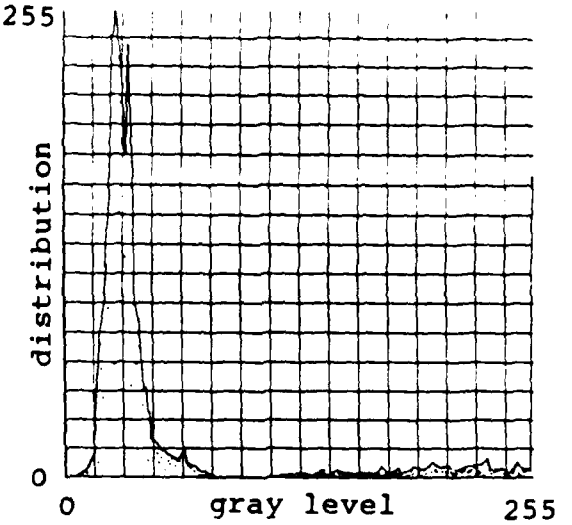

(d) Alphal = .1
Alpha2 = .4
Iter = 8

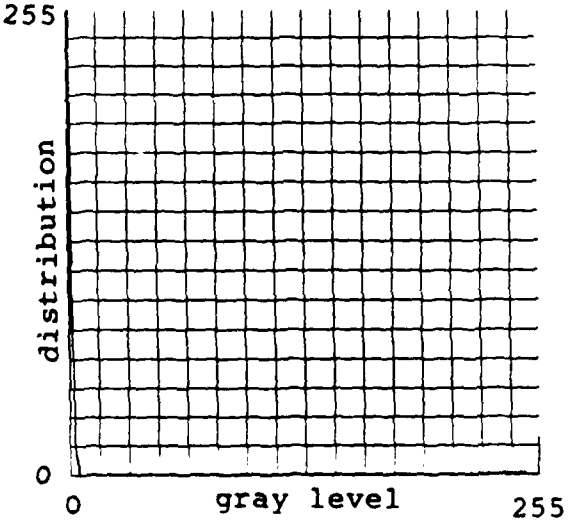

(Figure 4.5 continued)

TABLE 4.3
QUANTITATIVE RESULTS ON SAILBOAT

ALPHA1	ALPHA2	ITER	THD	REGION	AREA	PERIM	SHAPE
0.6	0.2	2	220	1	2309	526	8.78
0.6	0.2	2	108	1	2724	296	18.41
0.6	0.2	8	220	1	2883	301	19.16
0.6	0.2	8	108	1	2883	301	19.16
0.1	0.4	2	220	1	1051	382	5.50
0.1	0.4	2	108	1	2042	234	17.45
0.1	0.4	8	220	1	1488	366	8.13
0.1	0.4	8	108	1	1801	217	16.60

MEAN = 108

results also allow for the easy selection of a threshold value. This case, and the previous cases, have demonstrated that the selection of a threshold to determine the area and the size of the region can be chosen as the mean value of the original image without significantly changing the measured parameters. The images are uniform and homogeneous after eight iterations in each case. Gaps are seen in the first iteration (Figure 4.6(a)), but are filled in after eight iterations.

5. Series of Frames of Single Ship

a. Ship A (Figure 4.2(e))

This is the first of a series of six images (Figures 4.2(e)-(j) which depicts a ship at various orientations as the camera is rotating. This scene clearly shows the separation between the sky, sea, and target. The

(a) Alphal = .6
Alpha2 = .2
Iter = 2

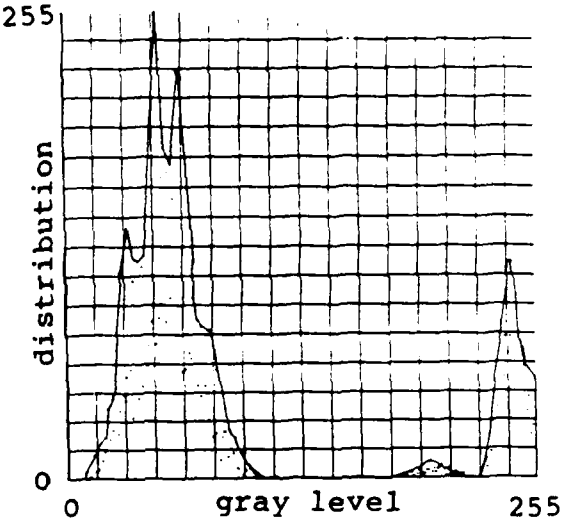

(b) Alphal = .6
Alpha2 = .2
Iter = 8

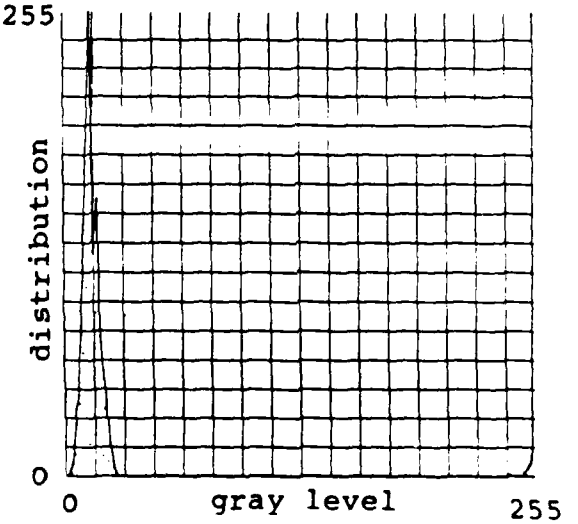

Figure 4.6: Results of relaxation segmentation on large ship

(c) Alphal = .1
Alpha2 = .4
Iter = 2

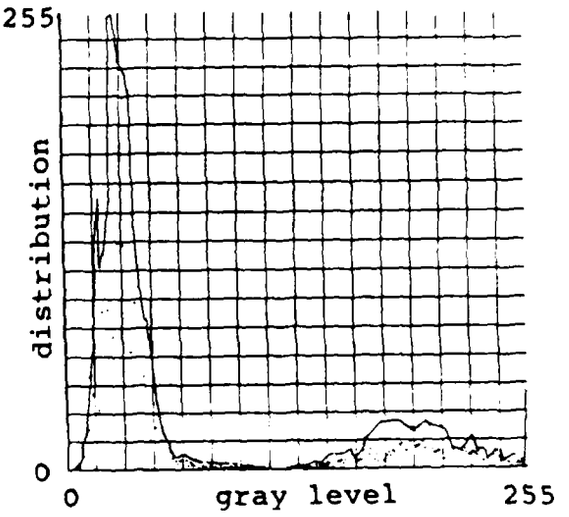

(d) Alphal = .1
Alpha2 = .4
Iter = 8

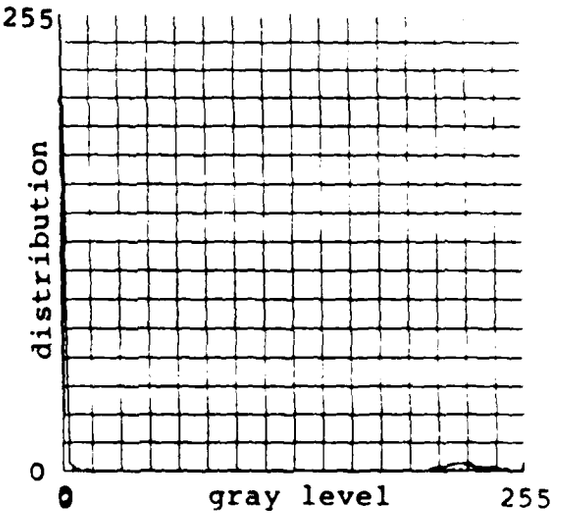

(Figure 4.6 continued)

TABLE 4.4
QUANTITATIVE RESULTS ON LARGE SHIP

ALPHA1	ALPHA2	ITER	THD	REGION	AREA	PERIM	SHAPE
0.6	0.2	2	220	1	3170	430	14.74
0.6	0.2	2	111	1	3450	332	20.78
0.6	0.2	8	220	1	3673	308	23.85
0.6	0.2	8	111	1	3679	307	23.97
0.1	0.4	2	220	1	248	139	3.57
0.1	0.4	2	111	3	2924	294	19.89
0.1	0.4	8	220	1	1687	534	6.32
0.1	0.4	8	111	2	2569	260	19.76

MEAN = 111

histogram shows three distinct peaks in the gray levels of Figure 4.2(e). Figure 4.7(a)-(e) shows the effect of the segmentation on this image. This case demonstrates how a high threshold and few iterations will segment image into several regions. When Alphal ≥ Alpha2, the target and the sky merge into one region after only two iterations. This prevents the detection and classification of the target. The situation becomes worse after eight iterations.

In the case where Alphal < Alpha2 (Figures 4.7(d)-(e)), the target is detectable after two iterations, but increasing the number of iterations creates the same result as the situation mentioned above; the sky and the target merge into one region. In this case, (see Figure 4.2(e)) the peak associated with the sky and the [illegible] greater than the mean, therefore these pixels were [illegible] together. This explains why these two areas [illegible]

AD-A184 666 AN APPLICATION OF A GRADIENT RELAXATION METHOD TO NOISY 2/2
INFRARED IMAGES(U) NAVAL POSTGRADUATE SCHOOL MONTEREY
CA J C MCDOUGALL JUN 87

UNCLASSIFIED F/G 17/5 1 NL

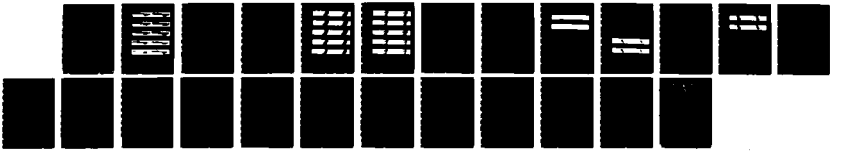

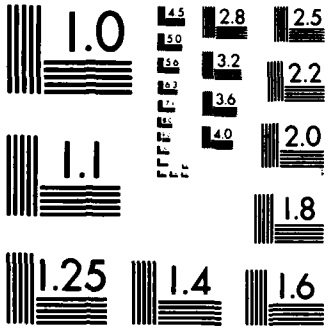

MICROCOPY RESOLUTION TEST CHART
NATIONAL BUREAU OF STANDARDS-1963-A

(a) Alphal = .3, Alpha2 = .3

(b) Alphal = .6, Alpha2 = .2

(c) Alphal = .4, Alpha2 = .1

(d) Alphal = .2, Alpha2 = .6

(e) Alphal = .1, Alpha2 = .4

Figure 4.7: Results of relaxation segmentation on Ship A

TABLE 4.5
QUANTITATIVE RESULTS OF SHIP A

ALPHA1	ALPHA2	ITER	THD	REGION	AREA	PERIM	SHAPE
0.3	0.3	2	220	6	49	34	2.88
0.3	0.3	2	120	2	6180	663	18.64
0.3	0.3	8	220	1	6139	625	19.64
0.3	0.3	8	120	2	6167	616	20.02
0.6	0.2	2	220	2	6012	7054	17.06
0.6	0.2	2	120	1	6935	768	18.06
0.6	0.2	8	220	1	7329	706	20.76
0.6	0.2	8	120	1	7366	697	21.14
0.4	0.1	2	220	3	3598	1088	6.61
0.4	0.1	2	120	1	7139	844	16.98
0.4	0.1	8	220	1	7475	680	21.99
0.4	0.1	8	120	1	7662	635	24.13
0.2	0.6	2	220	1	191	116	3.29
0.2	0.6	2	120	1	5488	692	15.86
0.2	0.6	8	220	1	5034	688	14.63
0.2	0.6	8	120	1	5069	712	14.24
0.1	0.4	2	220	1	698	189	7.39
0.1	0.4	2	120	1	5513	703	15.68
0.1	0.4	8	220	5	546	366	2.98
0.1	0.4	8	120	1	4749	675	14.07

MEAN = 120

together. If the pixels associated with the sky had been less than the mean, the target would have been grouped into its own region, permitting the detection and possible classification of the target. In general, the target is uniform and homogeneous, and gaps in the target region are eliminated. However, the desired shape of a ship does not occur with more iterations.

b. Ship B (Figure 4.2(f))

This is the second image in the series. The sky is to the left, the white region to the immediate left of the target is caused by glare, and the sea is to the right of the target. This effect is again due to the rotation of the sensor. Of the series of images seen in Figure 4.8(a)-(e), Figure 4.8(e) permits for the detection of a target and its orientation. The object cannot be classified in any of the cases. After eight iterations, the glare and the ship merge into one region as would be expected based on the two class segmentation scheme. This is a good example of how noise of similar intensity near or contained within the target can become merged as one region. This reduces the ability to classify the target. Quantitative results are shown in Table 4.6.

c. Ship C (Figure 4.2(g))

This image is similar to the previous case in that the background immediately surrounding the object has an intensity closely matching the object of interest. Figure 4.9 shows results of applying the relaxation segmentation technique. Figures 4.9(d) and (e) shows the cases that a target may be located in the area, or that a tremendous amount of glare from light reflected off the

(a) Alphal = .3, Alpha2 = .3

(b) Alphal = .6, Alpha2 = .2

(c) Alphal = .4, Alpha2 = .1

(d) Alphal = .2, Alpha2 = .6

(e) Alphal = .1, Alpha2 = .4

Figure 4.8: Results of relaxation segmentation on Ship B

(a) Alphal = .3, Alpha2 = .3

(b) Alphal = .6, Alpha2 = .2

(c) Alphal = .4, Alpha2 = .1

(d) Alphal = .2, Alpha2 = .6

(e) Alphal = .1, Alpha2 = .4

Figure 4.9: Results of relaxation segmentation on Ship C

TABLE 4.6
QUANTITATIVE RESULTS OF SHIP B

ALPHA1	ALPHA2	ITER	THD	REGION	AREA	PERIM	SHAPE
0.3	0.3	2	220	4	2324	476	9.76
0.3	0.3	2	144	1	3583	382	18.76
0.3	0.3	8	220	1	3589	367	19.56
0.3	0.3	8	144	1	3590	366	19.62
0.6	0.2	2	220	1	3568	406	17.58
0.6	0.2	2	144	1	3856	373	20.68
0.6	0.2	8	220	1	4087	349	23.42
0.6	0.2	8	144	1	4091	351	23.31
0.4	0.1	2	220	1	3315	438	15.14
0.4	0.1	2	144	1	3864	368	21.00
0.4	0.1	8	220	1	4199	385	21.81
0.4	0.1	8	144	1	4284	384	22.31
0.2	0.6	2	220	2	1407	402	7.00
0.2	0.6	2	144	1	3319	371	17.89
0.2	0.6	8	220	1	3064	312	19.64
0.2	0.6	8	144	1	3064	312	19.64
0.1	0.4	2	220	2	787	333	4.73
0.1	0.4	2	144	1	3319	382	17.38
0.1	0.4	8	220	1	2647	397	13.36
0.1	0.4	8	144	1	2895	321	18.04

MEAN = 144

the ocean surface (see Figure 4.2(g)). These last two cases clearly show that glare can have a degrading effect on the segmentation of the image of interest. Quantitative results are shown in Table 4.7.

d. Ship D (Figure 4.2(h))

This is a case where noise in the image can cause the object of interest to be obscured. Attempts to segment this image were unsuccessful (see Figure 4.10). By

TABLE 4.7
QUANTITATIVE RESULTS OF SHIP C

ALPHA1	ALPHA2	ITER	THD	REGION	AREA	PERIM	SHAPE
0.3	0.3	2	220	1	2021	483	8.37
0.3	0.3	2	174	1	2466	432	11.42
0.3	0.3	8	220	1	2558	370	13.83
0.3	0.3	8	174	1	2563	368	13.93
0.6	0.2	2	220	1	2495	462	10.80
0.6	0.2	2	174	2	2917	402	14.51
0.6	0.2	8	220	1	3263	425	15.36
0.6	0.2	8	174	1	3265	425	15.36
0.4	0.1	2	220	1	2466	481	10.25
0.4	0.1	2	174	1	2944	431	13.66
0.4	0.1	8	220	1	3365	437	15.40
0.4	0.1	8	174	1	3462	426	16.25
0.2	0.6	2	220	3	1397	450	6.21
0.2	0.6	2	174	1	2133	403	10.59
0.2	0.6	8	220	1	1824	334	10.92
0.2	0.6	8	174	1	1826	333	10.97
0.1	0.4	2	220	2	967	431	4.49
0.1	0.4	2	174	1	2081	431	9.66
0.1	0.4	8	220	1	1567	349	8.98
0.1	0.4	8	174	1	1604	335	9.58

MEAN = 174

increasing the number of iterations, the routine produced only fewer and smaller regions. Thus the algorithm could not provide information that an object may be within the frame of interest. This case clearly shows that the relaxation method fails in this situation. Quantitative results are shown in Table 4.8.

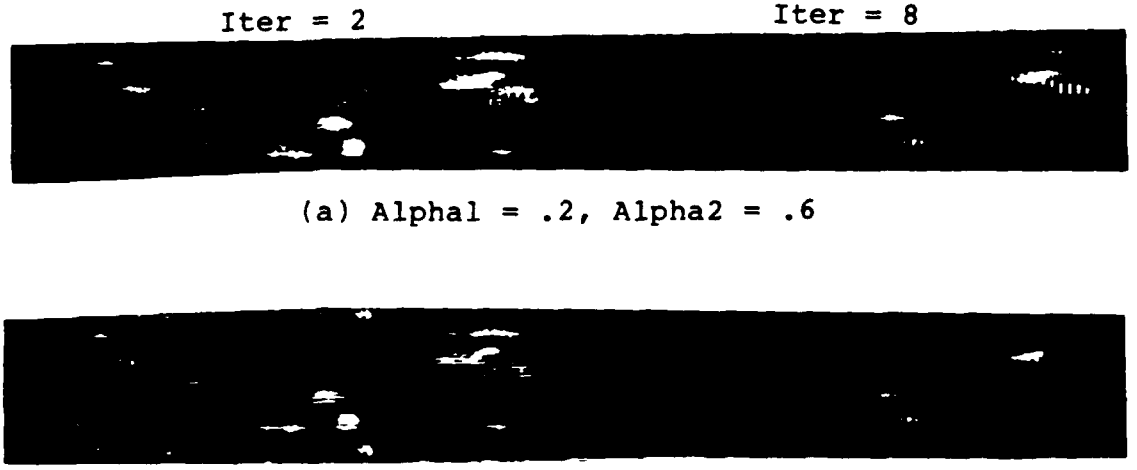

(a) Alphal = .2, Alpha2 = .6

(b) Alphal = .1, Alpha2 = .4

Figure 4.10: Segmentation of Ship D.

TABLE 4.8
QUANTITATIVE RESULTS OF SHIP D

ALPHA1	ALPHA2	ITER	THD	REGION	AREA	PERIM	SHAPE
0.2	0.6	2	220	5	64	44	2.91
0.2	0.6	2	153	8	308	188	3.28
0.2	0.6	8	220	2	75	39	3.84
0.2	0.6	8	153	2	75	39	3.84
0.1	0.4	2	220	5	53	47	1.75
0.1	0.4	2	153	8	293	178	3.29
0.1	0.4	8	220	1	45	45	2.00
0.1	0.4	8	153	1	62	36	3.44

MEAN = 153

e. Ship E (Figure 4.2(i))

This is the fifth image in the series for the same ship. Figure 4.11 and Table 4.9 shows the results of segmentation. This is a situation where a possible object may be in this frame. This case demonstrates that by increasing the number of iterations, the segmented region is more clearly defined by eliminating the noise near the object of interest. Also, more iterations reduces the number of segmented regions. The target is detected in the case. However, it does not allow for the classification of this target.

(a) Alphal = .2, Alpha2 = .6

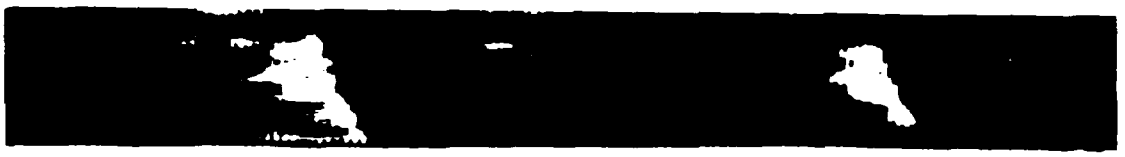

(b) Alphal = .1, Alpha2 = .4

Figure 4.11: Segmentation of Ship E

TABLE 4.9
QUANTITATIVE RESULTS OF SHIP E

ALPHA1	ALPHA2	ITER	THD	REGION	AREA	PERIM	SHAPE
0.2	0.6	2	220	5	950	241	7.88
0.2	0.6	2	189	5	1087	251	8.66
0.2	0.6	8	220	1	857	190	9.02
0.2	0.6	8	189	1	857	190	9.02
0.1	0.4	2	220	4	853	278	6.14
0.1	0.4	2	189	5	1042	249	8.37
0.1	0.4	8	220	1	699	151	9.26
0.1	0.4	8	189	1	727	161	9.03

MEAN = 189

f. Ship F (Figure 4.2(j))

The final image which was analyzed shows results (Figure 4.12 and Table 4.10) which are similar to hose seen in Figures 4.8 and 4.9. The glare which dominates the left side of the ship merges into the same region of the ship after only two iterations. It makes classification impossible and greatly reduces the possibility of detection. This case also demonstrates how several iterations can reduce the size of the segmented region. This case also demonstrates that by having a lower threshold value (i.e., the mean), there are fewer segmented regions (1 versus 6, or 1 versus 3), thus enabling an observer to focus on the one large region.

(a) Alpha1 = .2, Alpha2 = .6

(b) Alpha1 = .1, Alpha2 = .4

Figure 4.12: Segmentation of Ship F

TABLE 4.10
QUANTITATIVE RESULTS OF SHIP F

ALPHA1	ALPHA2	ITER	THD	REGION	AREA	PERIM	SHAPE
0.2	0.6	2	220	6	1222	318	7.69
0.2	0.6	2	171	1	2411	437	11.03
0.2	0.6	8	220	1	2055	361	11.39
0.2	0.6	8	171	1	2056	361	11.39
0.1	0.4	2	220	3	794	280	5.67
0.1	0.4	2	171	1	2341	430	10.89
0.1	0.4	8	220	1	1715	324	10.59
0.1	0.4	8	171	1	1797	331	10.86

MEAN = 171

C. SUMMARY OF RESULTS

The results show that for these cases, where the target has a high gray level and contains noise due to the environment and the sensor, it is best to have Alphal < Alpha2. This reduces the chance that noise which ahs gray levels greater than the mean will be included in the desired segmented region. Care must betaken to select appropriate values for Alphal and Alpha2, otherwise, the region will become so small that the object of interest is not classifiable. The target may still be detectable however. The result will provide the orientation of the target.

The process works well on an image which is similar to Figure 4.2(a). The peaks in the histogram are clearly defined and are sharp, not bell-shaped as in the case of the noisy images (Figures 4.1(b)-(j)). The noisy images can be segmented and generally identifiable if the target to be segmented is approximately ten percent or more of the frame of interest (Figures 4.2(b)-(e)). However, if the object occupies less than three percent of the image plane (Figure 4.2(h)), it is difficult or impossible, as in this case, to segment it by this method.

The segmented region in all cases was uniform, homogeneous, and any holes within the region were eliminated after several iterations. These are all desirable properties of in a segmentation routine. In summary, all

but one of the cases (Figure 4.2(h)) provided for the detection of a possible target, and four of the test images (Figures 4.3(a), (b), (c), and (d)) could be used as an input to a classification system.

V. CONCLUSION

Image segmentation is a critical step in the image analysis and pattern recognition process. Errors which occur at this step may propagate through additional stages of a pattern recognition system producing an incorrect description of the scene. The gradient relaxation technique is an iterative probability adjustment technique that can be used for segmentation. It takes advantage of both 'parallel' and the 'sequential' processing methods. The relaxation approach itself has two major advantages: 1) the classification decisions become better informed as the analysis proceeds, and 2) the method can use probabilistic classifications rather than making firm decisions immediately.

The approach is conducive to the segmentation problem of noisy infrared images having unimodal distributions. Noise near or within the target will be filtered out because each pixel's probability classification is adjusted based on the probabilistic classification of its neighbors. The gradient relaxation technique maximizes the gray level intensity of the target allowing for easier detection. The weighting factors must be chosen carefully. These factors are critical in determining the rate of convergence (length of

time to maximize the intensities), the extent that noise is eliminated from the image and the shape of the segmented region. The technique is still a subjective process and the ability of the observer to set the proper values of these factors is important.

The relaxation method is an ideal technique for region extraction because of its ability to sharpen the peaks in the histogram, create homogeneous and uniform regions, and the detected target conforms well to its original shape, i.e., a ship. This method is not suitable for edge detection of objects in noisy infrared images. The noise causes gaps in the edges at places where the transition between regions are not abrupt. Additional edges may be detected at points that are not part of the region boundaries.

Noisy images are primarily unimodal making the selection of a threshold difficult. This analysis showed that the threshold can be easily selected as the mean gray level intensity of the image. This allows for precious computational time to be spent for segmentation or other image processing, instead of being spent to search for a threshold for additional image analysis.

The technique is unable to separate noise of similar gray-level intensity near or within the target. This introduces errors into the image segmentation result, making

classification of the target difficult, if not impossible. The technique fails to segment targets which are not contiguous (i.e., broken up by the noise). The intended target either is segmented into several small regions or (if the intensity level of the noise is near that of the target) becomes part of the noise. This makes detection and classification of the target impossible.

This technique could be implemented in hardware as part of a signal processor. By implementing the technique as part of the processor, the requirements for an infrared sensor could be reduced. Possible requirements which would be reduced or eliminated include signal-to-noise ratio, detectivity and cooling requirements of the sensor, the weight and power for the system would possibly be reduced. Money saved in the cost of the sensor could be used to enhance the computing capabilities of the signal processor. Possible applications are missiles, remotely piloted vehicles (RPV's), aircraft, and remote sensors aboard spacecraft.

In summary, the gradient relaxation technique is a viable method to use in uncooled infrared sensors to detect targets. The ability of the technique to eliminate or reduce noise of intensity less than the target, thus enhancing the target and to provide for detection has been shown. The technique could possibly be used as one of the

inputs of a classification process (i.e., shape matching) or classification system, but only for those images where the intensity of the target is greater than that of the noise, or where the target has large spatial separation from the noise of similar intensity.

APPENDIX: EXPERIMENTAL PROCEDURE

The infrared images used in this analysis were obtained from an infrared uncooled focal plane array sensor. The images were then recorded and stored on a video disc. Using the EYECOM digitizing system, individual frames were extracted from the video disc. The EYECOM system creates an image file of 640 blocks of 512 bytes. This file must be reduced to 512 blocks of 512 bytes in order to be displayed on the COMTAL image processing system. This file was further reduced to 64 blocks of 256 bytes to reduce the processing time.

The measurements made in Chapter IV of the area and perimeter were obtained by calling subroutines in the Subroutine Package for Image Data Enhancement and Recognition (SPIDER) image processing package. The routines which were used are:

1. CLAB - The routine assigns labels (serial numbers) each segmented region. Each pixel in a region is assigned a label. This routine produces a labeled image.
2. AREA1 - The routine counts the number of pixels within every region in a labeled image.
3. PRMT1 - This routine measures the perimeter of every region in a labeled image. [Ref. 23]

LIST OF REFERENCES

1. Moick, Johannes G., Digital Processing of Remotely Sensed Images, pp. 1-5, 34-36, 227, NASA, 1980.

2. Schowengerdt, R. A., Techniques for Image Processing and Classification in Remote Sensing, p. 57. Academic Press, Inc., 1983.

3. Green, W. B., Digital Image Processing: A Systems Approach, pp. 1-2, 21, 50, Van Nostrand Reinhold Co., 1983.

4. Kunt, M., "Acquisition and Visualization," in Fundamentals in Computer Vision, O. D. Faugeras, Ed., pp. 1-26, Cambridge University Press, 1983.

5. Rosenfeld, A. and Kak, A. C., Digital Picture Processing, 2nd Ed., V. 2, pp. 55-56, 85, 145-150, 156, Academic Press, 1982.

6. Gonzales, R. C. and Wintz, P., Digital Image Processing, pp. 320-321, 345, Addison-Wesley Publishing Co., 1977.

7. Haralick, R. M., "Image Segmentation Survey," in Fundamentals in Computer Vision, O. D. Faugeras, Ed., pp. 209-223, Cambridge University Press, 1983.

8. Pavlidis, T., Structural Pattern Recognition, Springer-Verlag, p. 7, 1977.

9. Fu, K. S. and Mui, J. K., "A Survey on Image Segmentation," Pattern Recognition, V. 13, pp. 1-16, 1981.

10. Rosenfeld, A., "Iterative Methods in Image Analysis," IEEE Conference Proceedings on Pattern Recognition and Image Processing, pp. 14-18, June 1977.

11. Pavlidis, T., Algorithms for Graphics and Image Processing, p. 67, Computer Science Press, Inc., 1982.

12. Rosenfeld, A., Hummel, R. A. and Zucker, S. W., "Scene Labeling by Relaxation Operations," IEEE Transactions on Systems, Man, and Cybernetics, V. SMC-6, pp. 420-433, June 1976.

13. Zucker, S. W., "Relaxation Labeling and the Reduction of Local Ambiguities," Proceedings 3rd International Joint Conference on Pattern Recognition, pp. 852-861, 1976.

14. Rosenfeld, A., "Relaxation Methods in Image Processing and Analysis," 4th International Joint Conference On Pattern Recognition, pp. 181-185, 1978.

15. Bhanu, Bir and Gaugeras, O. D., "Segmentation of Images Having Unimodal Distributions," IEEE Transactions on Pattern Analysis and Machine Intelligence, V. PAMI-4, pp. 408-419, July 1982.

16. Hamming, R. W., Coding and Information Theory, 2nd ed., pp. 107-112, Prentice-Hall, 1986.

17. Faugeras, O. D., "Relational Structure Matching and Relaxation Labeling," in Fundamentals in Computer Vision, O. D. Faugeras, Ed., pp. 385-400, Cambridge University Press, 1983.

18. Bhanu, Bir, personal letter.

19. Rosen, J. B., "The Gradient Projection Method for Nonlinear Programming, Part I. Linear Constraints," Society for Industrial and Applied Mathematics Journal, V. 8, No. 1, pp. 181-217, March 1960.

20. University of Southern California Image Processing Institute Report 1030, Shape Matching and Segmentation Using Stochastic Labelling, by B. Bhanu, pp. 233-277, August 1981.

21. Otsu, N., "A Threshold Selection Method for Gray-Level Histograms," IEEE Transactions on Systems, Man, and Cybernetics, V. SMC-9, pp. 62-66, January 1979.

22. COMTAL Corp., COMTAL VISION ONE/20 Users Manual, 1980.

23. Joint Systems Development Program, Subroutine Package for Image Data Enhancement and Recognition (SPIDER) Users Manual, pp. II-48--50, III-19, -39, -390, 1983.

BIBLIOGRAPHY

Bhanu, B. and Faugeras, O. D., "Computer Analysis of Moving Images," in University of Southern California Image Processing Institute Report 960, Image Understanding Research, R. Nevatia and A. Sawchuk, Eds., March 1980.

Dorny, C. N., A Vector Space Approach to Models and Optimization, John Wiley and Sons, 1975.

Elliot, H. and Hansen, F. R., "Image Segmentation using Simple Markov Field Models," IEEE International Conference on Acoustics, Speech, and Signal Processing, pp. 1912-1915, May 1982.

Faugeras, O. D. and Berthrod, M., "Scene Labeling: An Optimization Approach," Proceedings IEEE Computer Society Conference on Pattern Recognition and Image Processing, pp. 318-326, August 6-8, 1979, Chicago.

Faugeras, O. D. and Berthrod M., "Using Context in Global Recognition of a Set of Objects: Optimization Approach," Proceedings of the 8th World Computer Congress (IFIP80), pp. 695-698, Tokyo.

Goos, G. and Hartmanis, J. Eds., Lecture Notes in Computer Science, V. 109, Digital Image Processing Systems, edited by L. Bolc and Z. Kulpa, Springer-Verlag, 1977.

Haralick, R. M. and Simon, J. C., Eds., Issues in Digital Image Processing, Sijthoff and Noordhoff, 1980.

Kanade, Takeo, "Region Segmentation: Signal vs. Semantics," 4th International Joint Conference On Pattern Recognition, pp. 95-105, 1978.

Keskes, N., Boulanouar, A. and Faugeras, O. D., "Applications of Image Analysis Techniques to Seismic Data," IEEE International Conference on Acoustics, Speech, and Signal Processing, pp. 855-857, May 1982.

Nagin, P., Hanson, A. and Riseman, E., "Studies in Global and Local Histogram-Guided Relaxation Algorithms," IEEE Transactions on Pattern Analysis and Machine Intelligence, V. PAMI-4, pp. 263-276, May 1982.

Rosenfeld, A. and Kak, A., Digital Picture Processing, 2nd Ed., V. 1, Academic Press, 1983.

Rosenfeld, A. Ed., Image Modeling, Academic Press, 1981.

Rosenfeld, A., "Image Understanding Project Status Report," Proceedings DARPA Image Understanding Workshop, pp. 14-24, April 1979.

Schater, Bruce J. and others, "An Application of Relaxation Methods to Edge Reinforcement," IEEE Transactions on Systems, Man, and Cybernetics, V. SMC-7, pp. 813-816.

Shafer, S. and Kanade T., "Recursive Region Segmentation by Analysis of Histograms," IEEE International Conference on Acoustics, Speech, and Signal Processing, pp. 1166-1171, May 1982.

Young, T. and Fu, K. Eds., Handbook of Pattern Recognition and Image Processing, Academic Press, 1986.

Zucker, Steven W., Hummel, Robert A. and Rosenfeld, A., "An Application of Relaxation Labeling to Line and Curve Enhancement," IEEE Transactions On Computers, V. C-26, pp. 394-403, April 1977.

INITIAL DISTRIBUTION LIST

	No. Copies
1. Defense Technical Information Center Cameron Station Alexandria, Virginia 22304-6145	2
2. Library, Code 0142 Naval Postgraduate School Monterey, California 93943-5002	2
3. Chairman, Electrical and Computer, Code 62 Engineering Department Naval Postgraduate School Monterey, California 93943	1
4. Professor Chin-Hwa Lee, Code 62LE Naval Postgraduate School Monterey, California 93943	3
5. Professor Charles W. Therrien, Code 62TI Naval Postgraduate School Monterey, California 93943	1
6. Commander U.S. Army Missile Command ATTN: AMSMI-RD-DP-TT Redstone Arsenal, Alabama 35898-5244	1
7. Commandant U.S. Army Space Institute ATTN: ATZL-SI Ft. Leavenworth, Kansas 66027-7300	1
8. Captain James C. McDougall 3304 Fillmore Avenue El Paso, Texas 79930	5

END

10-87

DTIC